NEANDC (E) - 222 U Vol. V
INDC (Ger) - 23 / L + Special
FIZ-KA--2

PROGRESS REPORT ON NUCLEAR DATA RESEARCH IN THE FEDERAL REPUBLIC OF GERMANY

for the Period April 1, 1980 to March 31, 1981

Fachinformationszentrum Energie Physik Mathematik

ISSN 0172–2204

1981

Nr. 2

NEANDC (E) - 222 U Vol. V
INDC (Ger) - 23 / L + Special
FIZ-KA--2

PROGRESS REPORT ON NUCLEAR DATA RESEARCH IN THE FEDERAL REPUBLIC OF GERMANY

for the Period April 1, 1980 to March 31, 1981

July 1981

Edited by
S. Cierjacks
Kernforschungszentrum Karlsruhe
Institut für Kernphysik
and
H. Behrens
Fachinformationszentrum Energie
Physik, Mathematik, Karlsruhe

FACHINFORMATIONSZENTRUM ENERGIE · PHYSIK · MATHEMATIK GMBH KARLSRUHE

December 1981, Nr. 2

ISSN 0172–2204

Vertrieb:

Fach-
informations-
zentrum
Energie
Physik
Mathematik GmbH
Karlsruhe

7514 Eggenstein-Leopoldshafen 2
Telefon (07247) 824600/01
Telex 7826487 fize d

Preis: 10,– DM (incl. MwSt.) + Porto

Printed in the Federal Republic of Germany

Druck:
Badendruck GmbH
Lammstraße 1–5
7500 Karlsruhe 1

Foreword

This report has been prepared to promote exchange of nuclear data research information between the Federal Republic of Germany and the other member states of NEA and IAEA. It brings together progress reports from KfK Karlsruhe, KFA Jülich, the Universities of Hamburg, Kiel, Köln, Darmstadt, Marburg and München, as well as from PTB Braunschweig and FIZ Karlsruhe. The emphasis in the works reported here has been on measurement, evaluation and compilation of application-oriented nuclear data, such as those relevant to fission and fusion reactor technologies, development of intense spallation neutron sources, production of medically important short-lived radioisotopes, etc.

Each contribution is presented under the laboratory heading where the work was done. If the work is relevant to requests in the World Request List for Nuclear Data, WRENDA 79/80 (INDC (SEC) - 73/URSF), the corresponding request identification numbers have been listed after the title and authors' names of the respective contribution.

Karlsruhe, July 1981

S. Cierjacks
H. Behrens

CONTENTS

KERNFORSCHUNGSZENTRUM KARLSRUHE
INSTITUT FÜR ANGEWANDTE KERNPHYSIK

1. 3 MV Van de Graaff-Accelerator

1.1 Neutron Total and Capture Cross Sections of the Stable Ne Isotopes

J. Almeida, D. Erbe, F. Käppeler

For this investigation, samples of natural neon and enriched ^{21}Ne and ^{22}Ne were used in high pressure gas containers. The total cross section was determined for neutron energies between 7 and 800 keV from a transmission experiment. With the time-of-flight (TOF) technique

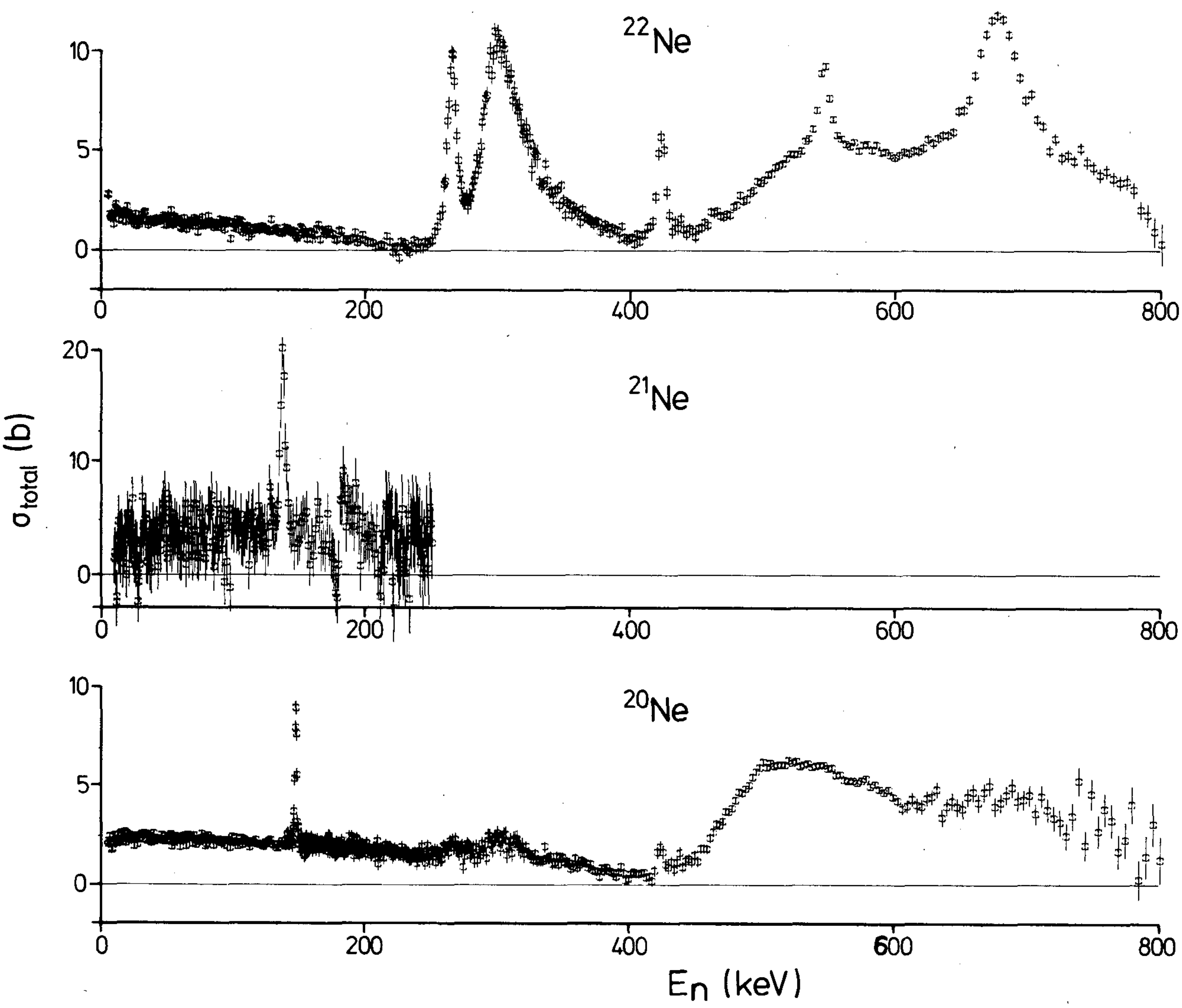

Fig. 1 Measured total cross sections of the stable neon isotopes.

a resolution of 0.5 ns/m was achieved at a flight path of 3 m. Data with good accuracy could be taken for ^{20}Ne and ^{22}Ne whereas only average information was obtained for ^{21}Ne due to the limited available sample mass. Fig. 1 shows the total cross sections as they were calculated from the measured transmission (see also Ref. 1).

The capture cross section measurement was carried out in the neutron energy range from 3 to 200 keV using C_6D_6 detectors. The samples were located at a flight path of 60 cm allowing for a TOF resolution of 2 ns/m. Great care was taken in optimizing neutron collimation and gamma ray shielding because for all neon isotopes only weak capture resonances were found. At present, data analysis is underway.

References

[1] J. Almeida, F. Käppeler, KFK-report 3068 (1980) 6.

1.2 Determination of the Capture Width of s-Wave Resonances in ^{56}Fe, $^{58,60}Ni$ and ^{27}Al

K. Wisshak, F. Käppeler, G. Reffo* and F. Fabbri*

(Relevant to request numbers: 762074, 692101, 692103, 692104, 714005, 741040, 753036, 762100, 792201, 761039, 741046, 692128, 692131, 702009, 741053, 753039, 762110, 792207, 792010, 741056, 741059)

The capture widths of s-wave resonances in ^{56}Fe (27.7 keV), ^{58}Ni (15.5 keV), ^{60}Ni (12.5 keV) and ^{27}Al (34.7 keV) have been determined using a setup completely different from previous experiments. A pulsed 3 MV Van de Graaff-accelerator and the $^{7}Li(p,n)$ reaction served as a neutron source. Capture gamma rays were observed by three Moxon-Rae detectors with different converter materials and gold was used as a standard. The samples were positioned at a flight path of 8.0 cm only. This allowed the use of very thin samples avoiding large multiple

---

*Comitato Nazionale Energia Nucleare, Bologna, Italy scattering corrections. Events due to capture of resonance scattered neutrons in the detector or surrounding materials were completely eliminated by time-of-flight.

The main systematic uncertainty in a relative measurement using Moxon-Rae-detectors is caused by deviations of the detector efficiency from the ideal linear increase with gamma ray energy. This holds especially in the present case as the capture gamma ray spectra of the samples and the reference sample are quite different. To reduce this uncertainty data were taken simultaneously from three detectors with different converter materials (graphite, mixed bismuth-graphite and pure bismuth). In addition detailed calculations of the capture gamma ray spectra have been performed in the framework of the statistical model taking advantage of all available experimental information (e.g. on level schemes, gamma decay branchings, level densities,cross sections etc.). These spectra together with the relative shape of the detector efficiency taken from literature allow to correct the data of each detector separately.

At present data evaluation is in progress.

1.3 Determination of the Capture Widths of Neutron Resonances in $^{56,58}Fe$ in the Energy Range from 10 to 100 keV

F. Käppeler, L.D. Hong, and K. Wisshak
(Relevant to request numbers: 692101, 692103, 692104, 714005, 741040, 753036, 762100, 792201, 741046, 691104, 762179)

The capture widths of s-wave resonances in ^{56}Fe and ^{58}Fe have been determined using a pulsed 3 MV Van de Graaff-accelerator and the $^{7}Li(p,n)$ reaction. The samples were positioned at a flight path of 60 cm, capture events were detected by two C_6D_6 detectors and gold was used as a standard cross section. In spite of the short flight path an energy resolution of 1.7 ns/m was obtained which was sufficient to perform a detailed resonance analysis. The distance from sample to detector was large enough compared to the primary flight path to discriminate background due to capture of resonance scattered neutrons by time of flight. In this way, e.g., the capture width of the broad s-wave resonances in ^{58}Fe (43.4 keV and 66.7 keV) could be determined with high accuracy. In Fig. 1 the experimental capture yield of ^{58}Fe is shown in the energy range from 36 to 70 keV. The solid line is the result of a shape analysis using the FANAC code of F. Fröhner.

During the experiments data were recorded from the two detectors in coincidence and anticoincidence mode. This allowed to deduce information on the relative gamma ray multiplicity for individual resonances, which possibly may be related to the respective resonance spins.

As data analysis is not yet finished completely, final resonance parameters and uncertainties can not be given. However, the statistical accuracy of the strong resonances is certainly better than 5 %.

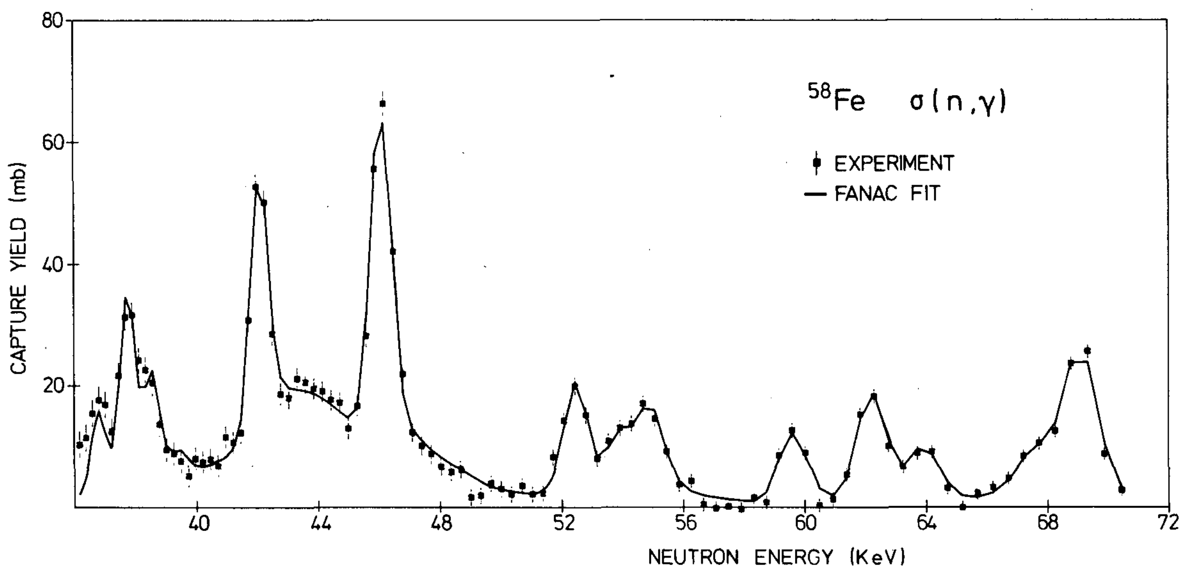

Fig. 1 Neutron capture cross section of ^{58}Fe

1.4 Capture Cross Section Measurements on Xe, Sm, Eu and Gd-isotopes with the Activation Method

H. Beer, F. Käppeler, G. Reffo*

(Relevant to request number: 741102)

The capture cross sections of $^{124,132,134}Xe(n,\gamma)$, $^{152}Sm(n,\gamma)$, $^{152}Eu(n,\gamma)^{152}Eu^{m}$ and $^{152,158,160}Gd(n,\gamma)$ have been determined at 25 keV relative to ^{197}Au as a standard using the activation technique. Neutrons were generated via the $^{7}Li(p,n)$ reaction just above the reaction threshold with a 3 MV Van de Graaff-accelerator. The resulting capture cross sections constitute with good approximation a Maxwellian average for a thermal energy of kT = 25 keV [1]. As in the keV energy range the capture cross sections are normally well-described by a 1/v-energy dependence, the Maxwellian average at kT = 25 keV is at the same time a good representation of the respective differential cross section at 25 keV [2].

The measurements were carried out with samples of natural isotopic composition except for ^{152}Gd which was enriched to 42.67 %. The samples for the xenon activations consisted of sodiumperxenat ($Na_4Xe\,O_6$) whereas the Eu and Gd samples were made of oxide powder. The compounds were pressed to self-supporting tablets of 6 mm diameter. The Sm sample was a metal foil of the same diameter.

The activated nuclei were counted with a Ge(Li) detector (42 cm^3, with an energy resolution of 2 keV at 1.33 MeV) via a strong characteristic gamma-ray line.

In Table I the results are summarized. As $^{132,134}Xe$, ^{152}Sm and $^{158,160}Gd$ are fission product nuclei their cross sections are of interest in reactor physics. The ^{151}Eu capture cross section to the 9.3 h isomeric level can be used to calculate the population of the isomeric state via keV neutron capture. A value of 0.41 $\pm$ 0.04 was derived for this probability adopting a ^{151}Eu total capture cross section of 4500 $\pm$ 240 mb at 30 keV. For the investigated isotopes no previous experimental work exists except for ^{152}Sm and $^{158,160}Gd$. Our ^{152}Sm

---

*Comitato Nazionale Energia Nucleare, Bologna, Italy

Table I Capture cross section measured by the activation technique compared to previous work

Target nucleus	σ(mb) at 25 keV		
	present work	other work	
^{124}Xe	1134±114		
^{132}Xe	69±4		
^{134}Xe	34±2		
^{152}Sm	440±27	411±71$^{1)}$	644±51$^{2)}$
^{151}Eu	2051±148*		
^{152}Gd	1144±71		
^{158}Gd	242±21		462±46$^{2)}$
^{160}Gd	159±15		227±44$^{2)}$

* cross section to the 9.3 h isomer in ^{152}Eu

$^{1)}$Macklin et al. [3] at 30 keV

$^{2)}$Kononov et al. [4] at 26 keV

cross section is in excellent agreement with the corresponding value given by Macklin et al. [3]. For ^{152}Sm and ^{158,160}Gd capture cross sections have also been reported by Kononov et al.[4]. These results are up to a factor of 2 higher than our values.

REFERENCES

[1] H. Beer, F. Käppeler, Phys. Rev. C21, 534 (1980).

[2] R.L. Macklin, J.H. Gibbons, Rev. Mod. Phys. 37, 166 (1965).

[3] R.L. Macklin, J.H. Gibbons, T. Inada, Nature 197, 369 (1963).

[4] V.N. Kononov, B.D. Yurlov, E.D. Poletaev, V.M. Timokhov, Sov. J. Nucl. Phys. 27, 5 (1978).

1.5 Fast Neutron Capture Cross Sections and Related Gamma Ray Spectra of ^{93}Nb, ^{103}Rh, and ^{181}Ta*

G. Reffo**, F. Fabbri**, K. Wisshak and F. Käppeler

(Relevant to request numbers: 621049, 682020, 753045, 762122, 762123, 712044, 732058, 691192)

The capture cross sections of ^{93}Nb, ^{103}Rh and ^{181}Ta were measured in the neutron energy range between 10 and 70 keV, using ^{197}Au as a standard. Most of the data points were obtained with a total uncertainty of ∿4 %. This was possible because of a detailed discussion of the systematic uncertainties involved. Extensive Hauser-Feshbach calculations were performed which yielded not only the neutron cross sections of the isotopes considered up to 4 MeV neutron energy but also partial capture cross sections and capture gamma ray spectra. For these calculations a consistent set of input parameters was determined from available experimental information or from empirical systematics. The effect of these parameters on the results is discussed.

---

* submitted for publication to Nucl. Sci. Eng.

**Comitato Nazionale Energia Nucleare, Bologna, Italy

1.6 A Double Energy - Double Velocity Measurement for Fragments from Fast Neutron Induced Fission of ^{235}U*

R. Müller**, A.A. Naqvi***, F. Käppeler, and F. Dickmann

We report on a complete (2E, 2v)-experiment for fast neutron induced fission on ^{235}U. The energy dependence of fragment properties so far known only for thermal neutron induced fission is studied. Experimental problems as well as difficulties in data analysis are considered in detail in order to obtain clean and unbiased results. In particular, a self consistent determination of the fragment kinetic energies TKE was achieved by comparing the results obtained via the respective velocities and pulse heights.
We find systematic discrepancies of 2 MeV if TKE is determined from the observed pulse heights using the calibration scheme of Schmitt et al. Therefore, refined calibration constants were deduced using accurate radiochemical mass yields.

Measurements were performed at neutron energies of 0.50 and 5.55 MeV. Our results include mean values of fragment properties before and after neutron evaporation e.g. of fragment velocities and masses, total kinetic energies, and the respective variances. We also show the distributions of fragment mass, of TKE and of the variance of TKE. In addition, the number of prompt fission neutrons ν is given as a function of fragment mass. Our mass resolution of 2.1 amu reveals fine structure not only in the fragment mass distribution but also in TKE (A*) and ν(A*).

For the lower neutron energy of 0.50 MeV the present results compare reasonably well with similar measurements performed with thermal neutrons. Apparently the 0.5 MeV increase in saddle point excitation does not alter the results significantly. The improved accuracy of this measurement is demonstrated by comparison of our neutron emission data with direct measurements of fission neutrons. At the higher neutron energy of 5.55 MeV we observe the expected decrease of shell and pairing effects which indicate an increase in nuclear temperature. These results are in qualitative agreement with the model of Wilkins, Chasman and Steinberg. However, a striking discrepancy exists for the number of fission neutrons where we find that the increase in the total number of fission neutrons is totally accounted for by heavy fragments alone.

*submitted for publication to Phys. Rev. C.

** Siemens AG, D-8000 München

*** Dept. of Physics, Univ. of Petrols and Minerals, Dhahran, Saudi-Arabia

1.7 The Isomeric Ratio in Thermal and Fast Neutron Capture of ^{241}Am*

K. Wisshak, J. Wickenhauser, F. Käppeler, G. Reffo** and F. Fabbri**

(Relevant to request numbers: 671135, 671136, 681807, 712108, 712109, 712110, 721099, 741127, 742108, 752033, 761098, 762153, 762170, 792228, 792230, 792231, 741142)

A new experimental method has been used to determine the isomeric ratio IR in neutron capture of ^{241}Am in a differential experiment. Thin ^{241}Am samples have been activated with monoenergetic neutrons of

14.75 meV and quasi monoenergetic neutrons of ∿30 keV. The decay of the ^{242g}Am nuclei produced has been determined by observing the emitted beta spectrum in a mini orange-spectrometer. The measurements have been performed relative to gold. The ratio $R_1 = \sigma_\gamma(^{241}\mathrm{Am} \rightarrow {}^{242g}\mathrm{Am})/\sigma_\gamma(\mathrm{Au})$ was found to be $R_1 = 5.79 \pm 0.33$ at 14.75 meV and $R_1 = 2.73 \pm 0.16$ at ∿ 30 keV. The corresponding isomeric ratios $IR = \sigma_\gamma(^{241}\mathrm{Am} \rightarrow {}^{242g}\mathrm{Am})/\sigma_\gamma(\mathrm{Am})$ are $IR = 0.92 \pm 0.06$ at 14.75 meV and $IR = 0.65 \pm 0.05$ at ∿ 30 keV.

Detailed theoretical calculations of the total capture cross section, the isomeric ratio and the capture gamma-ray spectra were performed in the energy range from 1 to 1000 keV taking advantage of recently available information on the discrete level scheme of ^{242}Am. With the present knowledge on the level scheme of ^{242}Am it seems to be difficult to reproduce the strong energy dependence of IR as indicated by the experimental results.

---

*submitted for publication to Nucl. Sci. Eng.

**Centro Nazionale Energia Nucleare, Bologna, Italy

2. Isochronous Cyclotron

2.1 High-Resolution Study of $^{16}O+n \rightarrow {}^{17}O(T=3/2)$ Resonances [x]

F. Hinterberger[1], P. v. Rossen[1], S. Cierjacks[2], G. Schmalz,
D. Erbe, B. Leugers

Sharp, isospin-forbidden, T=3/2 resonances have been studied using previously measured high-resolution total neutron cross sections of oxygen |1|. Total and partial widths and resonance energies were determined with high accuracy assuming narrow non-interfering multilevel Breit-Wigner resonances. A typical result of the resonance analysis is shown in Fig. 1.

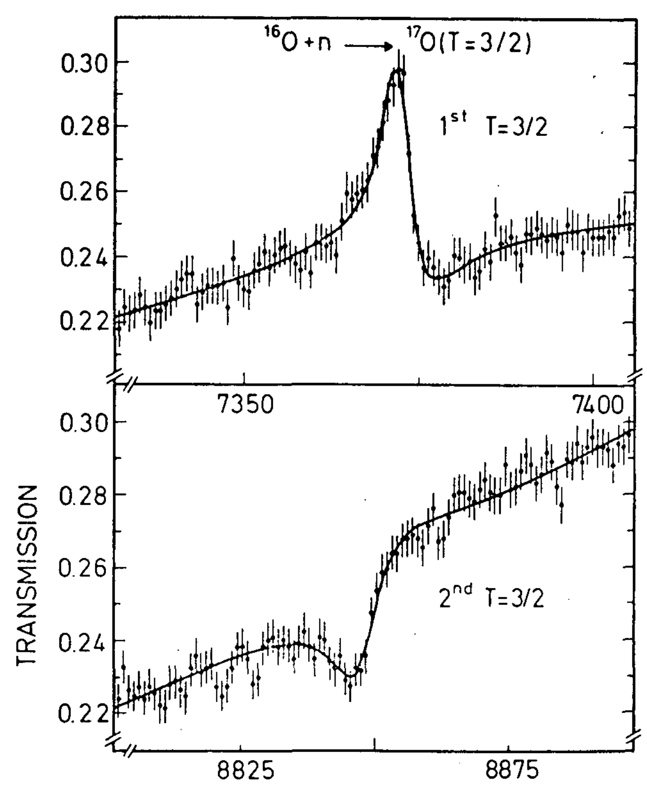

Fig. 1 Measured neutron transmission in the region of the first two $^{17}O(T=3/2)$ resonances. The solid lines are best-fit curves from a single-level resonance analysis

This figure displays the measured transmission data of the first two T=3/2 resonances in ^{17}O and best-fit curves obtained from a least squares fitting routine | 2 | . In Table 1 the resonance parameters for

---
[x] Nucl. Phys. A 352 (1981) 93

the first ten T=3/2 states derived from the present work are listed. For the 8th and the 9th T=3/2 state only a tentative total decay width Γ and an upper limit of $(J\pm 1/2)\ \Gamma_{n_o}$ could be derived from the experimental data. Employing the high-precision resonance energies for the low lying T=3/2 states in ^{17}O from this work and the energies of the analog states of the other members of the A-17 isospin multiplett from the literature |3| precise IMME parameters were derived. These were used in conjunction with the energies of the higher T=3/2 states in ^{17}N to predict the energies of additional T=3/2 states in ^{17}O. A search for sharp resonances anomalies at these energies in the total neutron cross sections provided the resonance parameters of other possible candidates for T= 3/2 states which are given in Table 2. Even though seven sharp resonances were found in the neighbourhood of the predicted energies their identification as isobaric analog states is still doubtfull, because of the lack of unambignous spin and parity assignments which need to be verified by additional experimental work.

TABLE 1
Resonance parameters of T=3/2 states in ^{17}O

Lab system E_n (keV)	c.m. system E_R (keV)	Γ (keV)	Γ_{n_o} (keV)	E_X (keV)	J^π a)
7373.31±0.18	6934.38±0.17	2.4±0.3	1.88±0.12	11078.7±0.8	$1/2^-$
8848.8±0.6	8321.7±0.6	6.9±1.1	1.27±0.14	12466.0±1.1	$3/2^-$
9353±6	8795.7±6	6±2 b)	0.21±0.14	12940±6	$1/2^+$
9414.9±0.6	8854.0±0.6	2.5±1.0	0.40±0.06	12998.3±1.0	$5/2^-$
10092.5±2.4	9491.0±2.3	9±5	0.24±0.09	13635.3±2.4	$(5/2^+)$
10725.5±1.5	10086.0±1.4	20.5±1.6	2.07±0.16	14230.3±1.6	$(7/2^-)$ c)
10785±3	10142±3	7.5±4	0.80±0.16	14286±3	
		10-50	≤0.5 d)	(15101±8) a)	
		10-50	≤0.5 d)	(16580±10) a)	$3/2^-$
14853±4	13966±4	46±12	1.9±0.6	18110±4	$3/2^-$

a) ref. |3|, b) constrained to the value of Adelberger et al. Phys. Rev. C 7 (1973) 889, c) tentative assignment of present work, d) upper limit for $(J\pm 1/2)\ \Gamma_{n_o}$

TABLE 2

Predicted neutron energies of other possible T = 3/2 states and sharp resonance anomalies found in ^{16}O neutron transmission

E_n^{pred} (keV)	E_n (keV)	Γ [a] (keV)	$(J+1/2)\,\Gamma_{n_o}$ (keV)	J^π [b]
	10960±3	40±6	13±6	
11247		(20)	$\leq$ 1	$9/2^-$
11283	11322±3	36±13	3.2±1.0	$1/2^-$
11541		(40)	$\leq$ 1	$\leq$ 7/2
11648	11756±3	52±14	11±3	(3/2)
11863	11936±3	40±6	7±1	$\leq$ 5/2
12083		(40)	$\leq$ 0.5	$\leq$ 7/2
12886	12867±4	21±10	2±0.5	$(7/2^+, 9/2^+)$
12913		(40)	$\leq$ 0.5	$(1/2, 3/2, 5/2)^+$
13252		(10-50)	$\leq$ 0.5	$3/2^-$ [c]
13524		(40)	$\leq$ 0.5	$\leq$ 7/2
13854		(40)	$\leq$ 0.5	
14024	14136±11	66±20	8.0±2.4	
14227		(40)	$\leq$ 0.5	
14418		(40)	$\leq$ 0.5	
14822	14853±4	43±12	1±0.3	$3/2^-$ [c]
	$\leq$ 15000	(40)	$\leq$ 1	

a) Values in paranthesis are used to evaluate an upper limit for $(J\underline{+}1/2)\Gamma_{n_o}$,

b) ref. |3|, c) assignment of Mairle et al., Nucl.Phys. A 280 (1977) 97

2.2 Experimental Study of Isospin Mixing in $^{12}C+n \rightarrow {}^{13}C$ (T=3/2) and $^{16}O+n \rightarrow {}^{17}O$ (T=3/2) Resonances [x]

S. Cierjacks[2], G. Schmalz[2], F. Hinterberger[1], P. v. Rossen[1]

Narrow resonances of the ^{12}C+n and the ^{16}O+n systems measured previously in high-resolution transmission experiments at the Karlsruhe isochronous cyclotron |1| have been used to study isospin mixing in low lying T=3/2 states. Resonance analyses of the transmission data provided precise total and partial decay widths and resonance energies for numerous narrow states of both isospins, T = 1/2 and T = 3/2. These data in conjunction with existing information on broad ^{13}C and ^{17}O (T=1/2) resonances |3,4| provided a good means to experimentally determine isospin mixing matrix elements employing the method proposed by Weigmann et al. |5|. By this method meningful results could only be derived for the first five T = 3/2 resonances in ^{17}O and the first T = 3/2 resonance in ^{13}C. The results of this work are listed in Table 3 in terms of the fractional admixture $\Gamma(T=3/2)/\overline{\Gamma}(T=1/2)$ and the two estimates of the average isospin mixing matrix elements, i.e. the zero's order guess $<\overline{T=3/2|V|i>}_o$ and the lower limit value $<\overline{T=3/2|V|i>}_{min}$. The comparison with other experimental results for isospin-forbidden neutron decays |5,6| shows that the zero's order guess is - with one exception - almost independant of the target mass and the J^π value in accordance with some shell model predictions. Possible consequences of this observation on the dominating isospin mixing mechanisms have been discussed.

2.3 Absolute Fission Cross Section Measurements Relative to the n,p-Standard

S. Cierjacks[2]

A survey of recent developments in absolute fission cross section measurements employing the n,p scattering cross section was prepared and presented at the X. International Symposium on Selected Topics of Fast Neutrons and Heavy Ions with Atomic Nuclei in Gaussig, Nov. 1980.

---

[x] Work presented at the 5th Nat. Sov. Conf. on Neutron Physics, Kiev, Sept. 1980

[1] Institut für Strahlen- und Kernphysik der Universität Bonn

[2] Now at Kernforschungszentrum Karlsruhe, Institut für Kernphysik

TABLE 3

Isospin impurities and isospin mixing matrix elements of T=3/2 resonances

System	J^{π} E (keV)	$\Gamma(3/2)/\overline{\Gamma}(1/2)$ (%)	$\overline{<T=3/2 \vert V \vert i>}_{o}$ (keV)	$\overline{<T=3/2 \vert V \vert i>}_{min}$ (keV)
$^{12}C+n$ a)	$J=3/2^-$ $E_r=10160.0$	0.62	152	37
$^{16}O+n$ a)	$J=1/2^-$ $E_r=6934.38$	3.6	231	111
$^{16}O+n$ a)	$J=3/2^-$ $E_r=8321.7$	0.54	174	56
$^{16}O+n$ a)	$J=1/2^+$ $E_r=8795.7$	0.16	135	47
$^{16}O+n$ a)	$J=5/2^-$ $E_r=8854.0$	2.9	340	154
$^{16}O+n$ a)	$J=(5/2^+)$ $E_r=9419.0$	1.3	166	16
$^{24}Mg+n$ b)	$J=5/2^+$ $E_n=475.4$	2	97	23
$^{24}Mg+n$ b)	$J=3/2^+$ $E_n=555.4$	2	(12)	7
$^{24}Mg+n$ b)	$J=1/2^+$ $E_n=1567.$	18	150	90
$^{28}Si+n$ c)	$J=1/2^+$ $E_n=1254.$	18	144	97

a) this work b) ref |5| c) ref. |6|

References

1 S. Cierjacks, F. Hinterberger, G. Schmalz, D. Erbe, P. v. Rossen, B. Leugers; High-Precision Time-of-Flight Measurements of Neutron Resonance Energies in Carbon and Oxygen between 3 and 30 MeV, Nucl. Instr. and Methods 169 (1980) 185

2 F. Hinterberger, P. v. Rossen, H.G. Ehrlich, B. Schüller, R. Jahn, J. Bisping, G. Welp; $^{12}C+p \rightarrow {}^{13}N$ (T=3/2) Resonance at 14.23 MeV; Nucl. Phys. A 253 (1975) 125

3 F. Ajzenberg-Selove; Energy Levels of Light Nuclei A = 16-17; Nucl. Phys. A 281 (1977) 1

4 F. Ajzenberg-Selove; Energy Levels of Light Nuclei A = 13-15; Nucl. Phys. A 268 (1976) 1

5 R. Weigmann, R.L. Macklin, J.A. Harvey; Isobaric Analog Impurities from Neutron Capture and Transmission by Magnesium, Phys. Rev. C 14 (1976) 1328

6 S. Cierjacks, S.K. Gupta, I. Schouky; Isobaric Analog Impurity from Total and Differential Neutron Scattering Cross Sections of Silicon; Phys. Rev. C 17 (1978) 12-17

KERNFORSCHUNGSZENTRUM KARLSRUHE
INSTITUT FÜR KERNPHYSIK

1. SIN Cyclotron

1.1 Neutron and Charged-Particle Production Yields and Spectra from Thick Metal Targets by 590 MeV Protons

S. Cierjacks, M.T. Rainbow [1], F. Raupp, M.T. Swinhoe [2], S.D. Howe, Y. Hino, L. Buth [3]

The measurements of angular and depth dependent neutron and charged-particle yields and spectra from thick heavy metal targets were continued. The data evaluation for thick lead targets at the angles 30°, 90° and 150° has been completed (1, 2, 3). In Fig. 1 the spectra of neutrons emitted from the first 5 cm target block are shown for 30°, 90°, and 150°. All three spectra exhibit the typical two-component shape due to evaporation and cascade neutrons (the latter of which produce the broad shoulder around 50 MeV). As expected the high energy component is most pronounced for neutron emission at 30°, and decreases rapidly with increasing emission angle. In the mean time similar measurements were carried out for a thick uranium target. The analysis of the four-parameter time-of-flight data is almost completed.

1.2 Measurement of the Neutron Detection Efficiency for an NE 213 Liquid Scintillator in the Region 50 to 450 MeV

S. Cierjacks, M.T. Swinhoe [2], L. Buth [3], S.D. Howe, F. Raupp

The average neutron detection efficiency of a 4.5 cm diameter, 3 cm thick, NE 213 liquid scintillator has been measured in the neutron energy region from 50 to 450 MeV for a wide range of threshold values. The knowledge of precise efficiencies was an important prerequisite for absolute neutron spectrum measurements performed as part of the project study for a new German spallation neutron source (comp. sections 1.1, 1.3, 2.1). For efficiency measurements the Freiburg University neutron facility at SIN (4) was employed. At this facility a large liquid-hydrogen target was available. The measurements were performed by use of the associated particle method. Equal numbers of neutrons and protons were produced at kinematically related angles by elastic

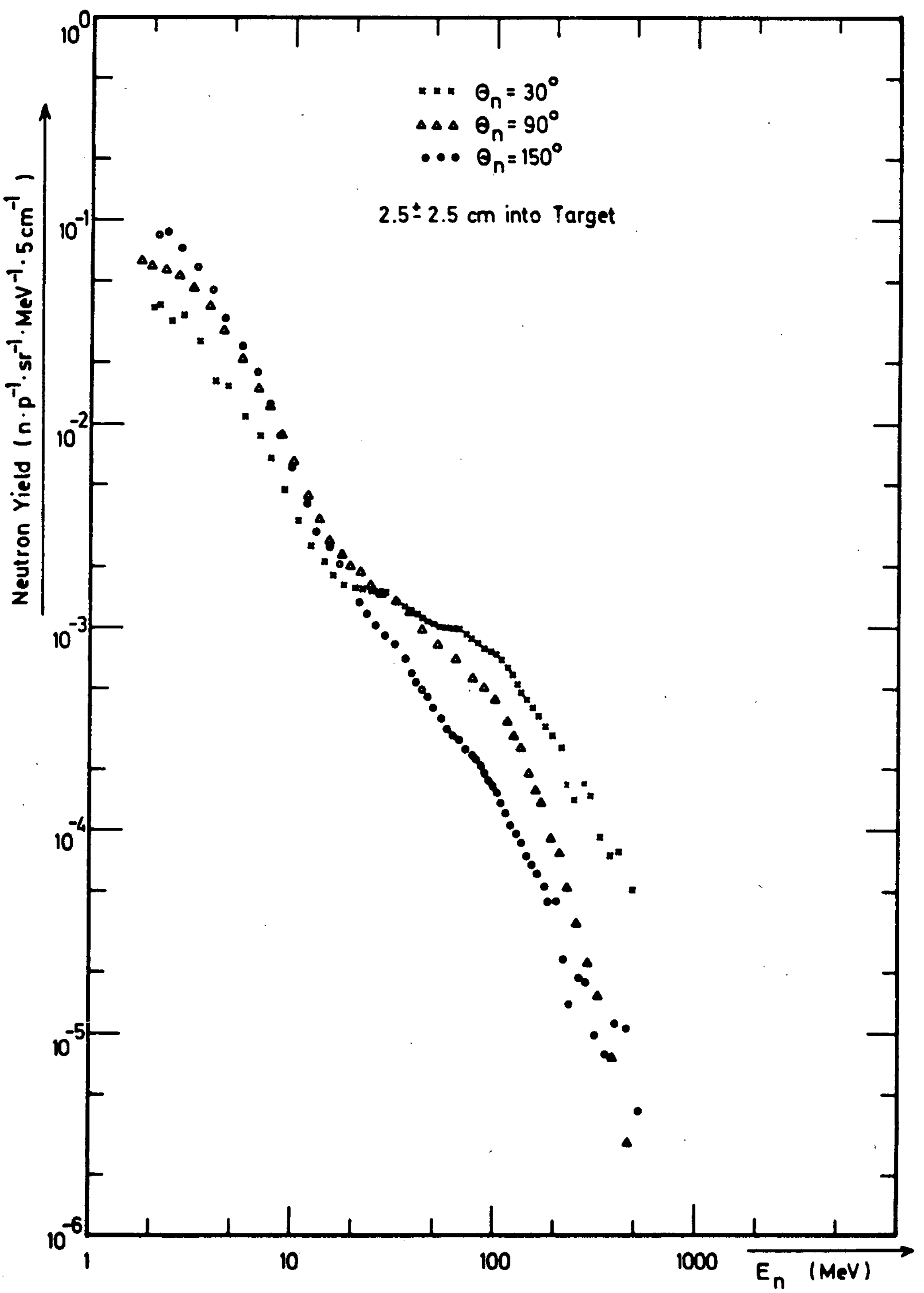

<u>Fig. 1:</u> Differential spectra of neutrons at 30°, 90°, and 150° from the first 5 cm of the 10 cm diameter lead target for an incident proton energy of 590 MeV.

scattering of neutrons from the liquid hydrogen target. The results of the measurement at detector thresholds of 0.6, 4.2 and 17.5 MeV_{ee} are shown in Fig. 2. The experimental data points are compared with calculated efficiencies obtained with the Monte Carlo program of Stanton (5) modified by Cecil et al. (6). The agreement between measured and calculated efficiencies is good for all three threshold values.

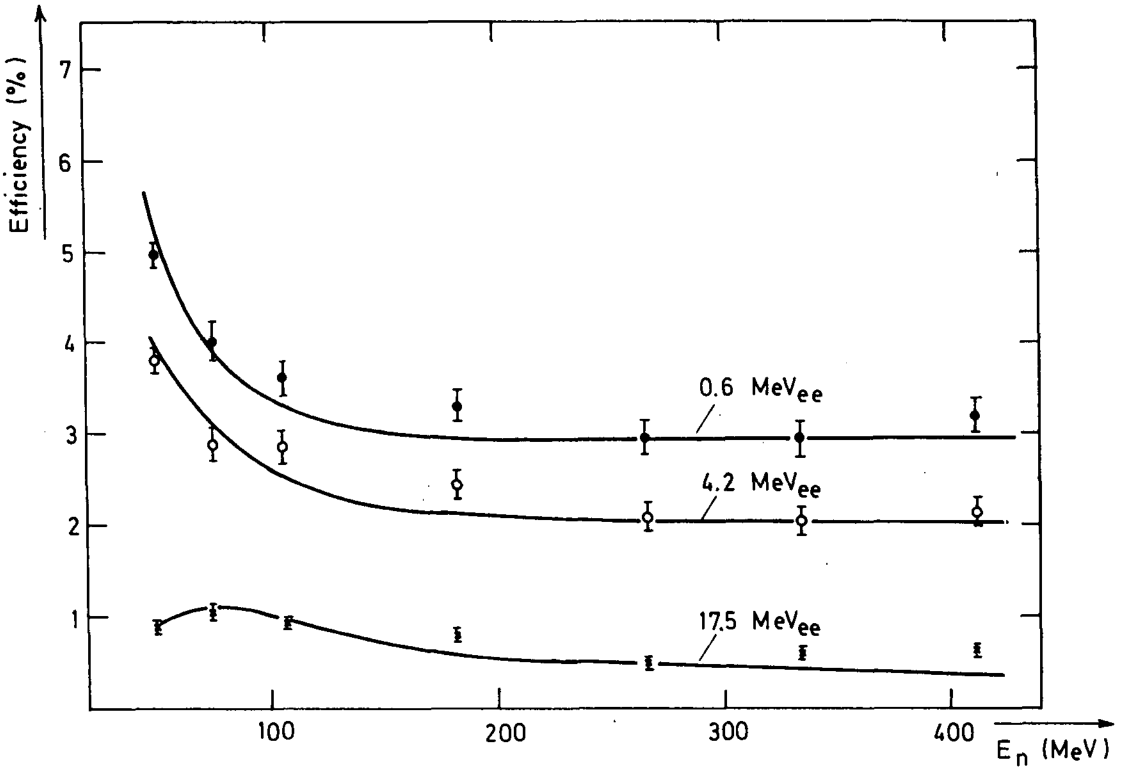

Fig. 2: Measured and calculated neutron detection efficiencies for a 4.5 cm diameter, 3.0 cm thick, NE 213 liquid scintillator

1.3 Measurements of Charged-Particle and Neutron Production Cross Sections for 590 MeV Protons

S. Cierjacks, S.D. Howe, Y. Hino, F. Raupp, L. Buth [3]

Angular dependent charged-particle and neutron production cross sections for 590 MeV protons were measured for C,Al, Fe, In, Ta, Pb and U. For charged-particles measurements were performed at emission angles of 23°, 45°, 90°, 135°, and 157° with time-of-flight resolutions ranging between 0.15 and 0.35 ns/m. In the neutron production cross section measurements the corresponding resolution was typically 0.4 ns/m, and data were taken at angles of 30°, 90°, and 150°. For both types of measurements thin samples, a few mm thick, were used. A first result for charged-particles is shown in Fig. 3.

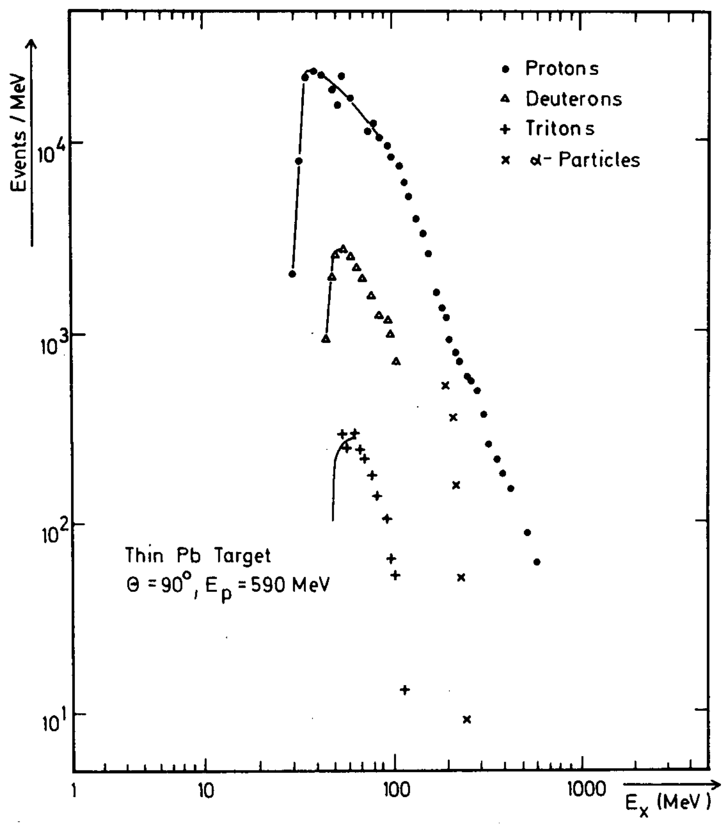

Fig. 3:

Spectral distribution of secondary charged-particles emitted at 90° from a 5.5 gr/cm^2 lead target bombarded by 590 MeV protons.

This diagram displays the spectral distribution of secondary protons, deuterons, tritons and α-particles emitted at 90° from a 5.5 gr/cm^2 lead target. Since this result stems from an early test experiment the time-of-flight resolution and low energy cut-off values were not yet optimum as in the main experiment. The data analysis of charged-particle and neutron production cross sections from the main experiment is presently underway.

2. SATURNE Accelerator

2.1 Angular and Depth Dependent Neutron and Proton Yields from Thick Metal Targets by 1100 MeV Protons

S. Cierjacks, M.T. Swinhoe [2], M.T. Rainbow [1], F. Raupp, S.D. Howe, Y. Hino, L. Buth [3]

In continuation of the previous studies with 590 MeV protons angular and depth dependent yields of neutrons and protons from thick targets were also measured for 1100 MeV incident protons. The extension of the program to higher energies was closely related to the SNQ reference concept, established in early 1980, which favoured a 5 mA, 1100 MeV accelerator rather than a 10 mA, 600 MeV machine.

For the measurements at 1100 MeV the whole experimental equipement was transferred from the SIN cyclotron to the synchrotron of the Laboratoire National SATURNE (LNS) at Saclay, France. First experiments carried out during the reporting period concentrated on yield and spectra measurements from thick lead and uranium targets at 90^{o}. Data analysis has been completed for part of the measurements. Extrapolations of the evaluated data to the whole target length and 4π confirm mainly the previously measured increase of total m/p-values with increasing proton energy (7). However, the measured spectra revealed a similar discrepancy with theoretical calculations as found for 590 MeV protons: Above ~ 100 MeV the high energy tails of the measured spectra are almost by an order of magnitude higher than the yields predicted by the HETC code (8).

2.2 Measurement of the High-Energy Component of the Neutron Spectrum from Moderated Sources

S. Cierjacks, Y. Hino, M.T. Swinhoe [2], M.T. Rainbow [1], S.D. Howe, F. Raupp, L. Buth [3]

The previous program of high energy spectra measurements by means of an unfolding method of analog spectra was extended to other target configurations and higher proton energies. Since the new detector array described in the previous progress report (9) was not available before the end of 1980, most of the new measurements were performed using the earlier standard method which is restricted to neutron energies below ~ 140 MeV. Some typical results obtained for target configurations and primary proton energies considered in the SNQ project study are shown in Fig. 4. Absolute neutron fluxes are given for a distance of 6 m from the source and for proton currents extrapolated to 5 mA (1100 MeV protons) and 10 mA (590 MeV protons), typical for two recent SNQ concepts.

At the end of the year the new detector array, involving a 30 cm long NE 213 liquid scintillator, became available. Its capability in conjunction with a FERDOR analysis (10) of the analog spectra was tested by measuring the same neutron spectrum from a bare lead target both by spectrum unfolding and by time-of-flight. It could be shown that the new unfolding method provides accurate results over an extended energy region from about 1 - 250 MeV. Beginning of 1981 the new system has been used to remeasure the high energy neutron spectrum from a moderated source consisting of a lead primary target, a polyethelen moderator and a lead reflector. The data analysis is nearly completed.

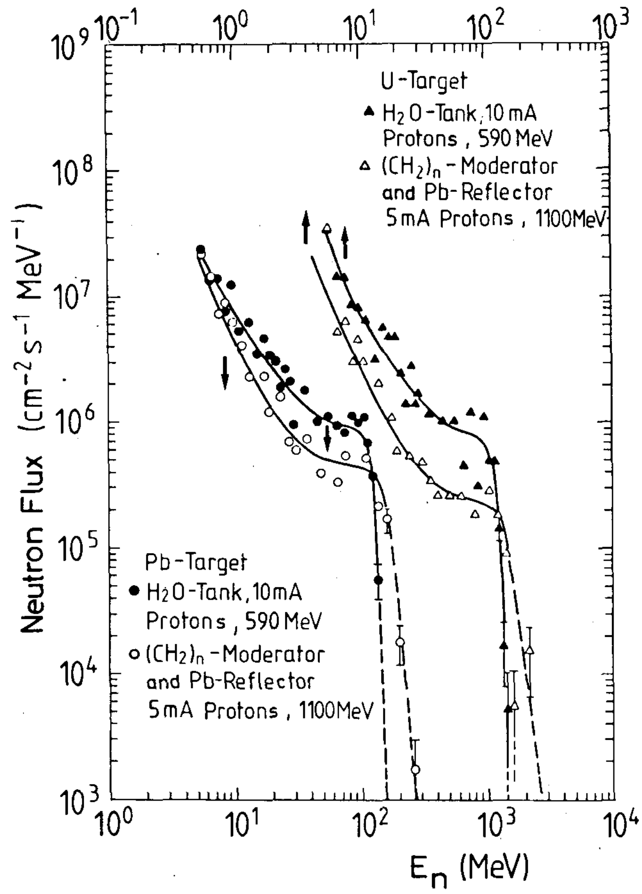

Fig. 4: High energy neutron spectra from moderated sources for several target configurations bombarded by 590 and 1100 MeV protons.

---

1 Present address: Physics Division, A.A.E.C. Research Establishment, Sutherland 2232, N.S.W., Australia

2 Present address: Nuclear Physics Division, AERE Harwell, Oxfordshire, OX11 ORA, United Kingdom

3 Permanent member of the Institut für Neutronenphysik and Reaktortechnik, Kernforschungszentrum Karlsruhe GmbH

References

(1) S. Cierjacks, M.T. Rainbow, M.T. Swinhoe, L. Buth; Neutron Yields and Spectra from 590 MeV (p,n) Reactions on Lead Targets, Proc. Symp. on Neutron Cross Sections from 10 to 50 MeV, BNL, May 1980, BNL-NCS-51245, Vol I p. 201 - 212

(2) S. Cierjacks, M.T. Rainbow, M.T. Swinhoe, L. Buth; Angular and Depth Dependent Neutron Yields and Spectra from 590 MeV (p,n) Reactions in Thick Lead Targets. Proc. 5th Nat. Conf. on Neutron Physics, Kiev, Sept. 1980, Vol 1, p. 269 - 284

(3) S. Cierjacks, M.T. Rainbow, M.T. Swinhoe, L. Buth; Neutron and Charged-Particle Production Yields and Spectra from Thick Metal Targets by 590 MeV Protons; ICANS-IV Meeting, Tsukaba, Japan, Oct. 1980; KfK-3097B, Dec 1980

(4) Th. Fischer, W. Hagedorn, G. Gammel, W. Fürster, K. Kern, P. Kettle, M. Kleinschmidt, L. Lehmann, K. Moser, E. Rössle , H. Schmitt, SIN Jahresbericht, E31, 1979

(5) N.R. Stanton, Ohio State University Report COO-1545-92, 1971

(6) R.A. Cecil, B.D. Anderson, R. Madey, Improved Predictions of Neutron Detection Efficiency for Hydrocarbon Scintillators from 1 to about 300 MeV, NIM 161 (1979) 439

(7) J.S. Fraser, R.E. Green, J.W. Hilborn, J.L.D. Milton, W.A. Gibson, E.E. Gross, A. Zucker; Neutron Production in Thick Targets Bombarded by High Energy Protons, Phys. in Canada 21 (2), 17 (1965)

(8) HETC - ORNL - 4744, Oak Ridge National Laboratory

(9) Progress Report on Nuclear Data Research in the Federal Republic of Germany for the Period April 1, 1979 for March 31, 1980, NEANDC(E)-212 U Vol. V, June 1980, p. 23

(10) W.R. Burrus, Report ORNL-3743, Oak Ridge National Laboratory, 1965

KERNFORSCHUNGSZENTRUM KARLSRUHE

INSTITUT FÜR KERN- UND TEILCHENPHYSIK

Isochronous Cyclotron

1. The Total Neutron Cross Section of the Boron Isotopes

M.S. Abdel-Wahab[+], D. Eversheim[++], F. Hinterberger[++], J. Kecskemeti, H.O. Klages, G. Schmalz

The total neutron cross section of the boron isotopes ^{10}B and ^{11}B was measured in the energy range from 1.5 to 40 MeV. The 190 m long flight path was used in high resolution measurements to look for isospin-forbidden resonances in the compound nuclei.

The acchieved energy resolution was better than $2 \cdot 10^{-4} * E^{1/2}$ (MeV). The analysis of the data is performed using a multi-level Breit-Wigner approach assuming noninterfering resonances and a slightly energy dependent background.

+ Now at Ain Shams University, Kairo

++ Institut für Strahlen- und Kernphysik, Universtät Bonn

2. Search for $^{20}Ne+n \rightarrow$ ^{21}Ne (T=3/2) resonances*

M.S. Abdel-Wahab[+], D. Eversheim[++], F. Hinterberger[++], J. Kecskemeti, H.O. Klages, G. Schmalz

The total neutron cross section of ^{20}Ne has been studied in the energy range 1.5 - 40 MeV using the 190 m neutron time-of-flight facility of the Karlsruhe Isochronous Cyclotron. The high resolution of 5.5 psec/m enables the study of sharp isospin forbidden resonances in ^{21}Ne with an effective energy resolution of about 4000:1. The first and fourth ^{21}Ne T=3/2-levels have been observed as weak anomalies allowing the precise determination of the total width Γ, the partial widt Γ_{n_o}, and the resonance energy E_R. Upper limits for the partial decay widths are deduced for those T=3/2-levels which do not appear as resonance anomalies.

The information deduced from the data permits a comparison of the resonance parameters of analogous T=3/2 states in mirror nuclei with A=4n+1 and a discussion of the possible charge dependence of T=1/2 inpurities in the T=3/2-levels.

* Work will be submitted for publication in Nuclear Physics

\+ Now at Ain Shams University, Kairo

++ Institut für Strahlen- und Kernphysik, Universtät Bonn

KERNFORSCHUNGSZENTRUM KARLSRUHE
INSTITUT FÜR NEUTRONENPHYSIK UND REAKTORTECHNIK

1. Nuclear Data Evaluation

1.1 Neutron Cross Sections of Actinides

B. Goel, H. Jahn, F.H. Fröhner

(Relevant to request numbers 691262, 691263, 702025, 691286, 692385, 714016, 732113, 781193, 691336, 681805, 681806, 712106, 792169, 681807, 681808, 752032, 792230, 792229, 792257, 792171, 792258, 712113, 711806, 792236, 762174, 792259, 732109)

The evaluation of ^{241}Am neutron cross sections for KEDAK is completed. The most recent KfK capture data in the keV region [1] are in very good agreement with the recommended KEDAK capture cross section curve that was calculated from level statistics obtained in the resolved resonance range and slightly adjusted to previously published average cross section data for higher energies (Fig. 1). The recommended fission cross section, calculated from the same level statistics (which include fission barrier characteristics reproducing the fission data of Behrens and Browne [2]) are quite compatible with recent measurements [1, 3], except perhaps in the shallow subthreshold minimum between about 50 and 200 keV where they are lower by 10 to 20% than the lowest experimental data (Fig. 2). The evaluation of ^{242m}Am, ^{243}Am and ^{244}Cm is in progress, nearing completion.

References

[1] K. Wisshak and F. Käppeler, Nucl. Sci. Eng. 76(1980)148

[2] J.W. Behrens and J.C. Browne, UCID-17324, Lawrence Livermore Laboratory (1976)

[3] W. Hage, K. Wisshak and F. Käppeler, Nucl. Sci. Eng. (accepted for publication)

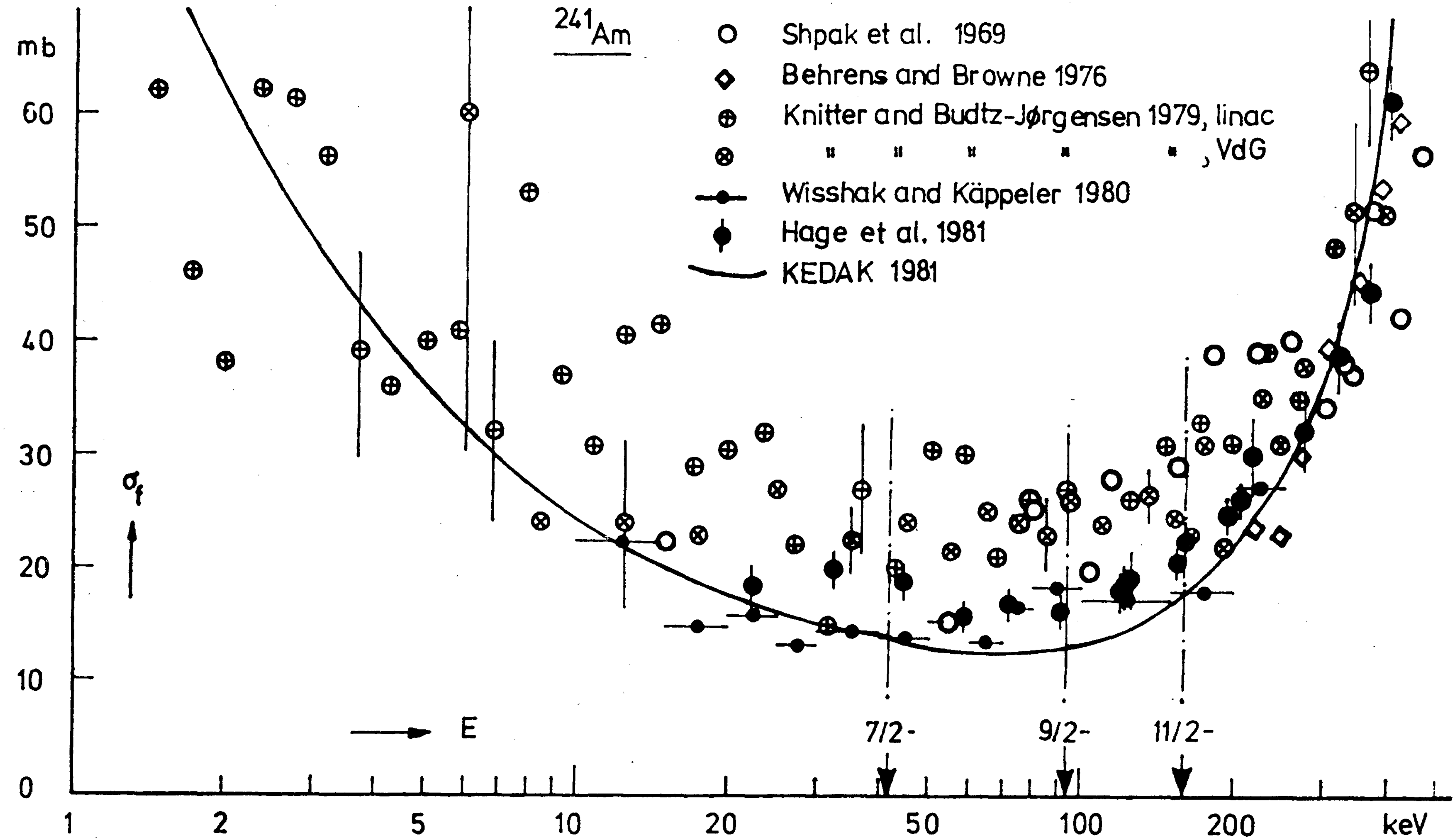

Fig. 2 - Measured and calculated fission cross sections for ^{241}Am+n in the subthreshold region. The first three inelastic thresholds, where the level-statistically calculated KEDAK curve is discontinuous, are indicated by arrows and the spins and parities of the residual excited levels.

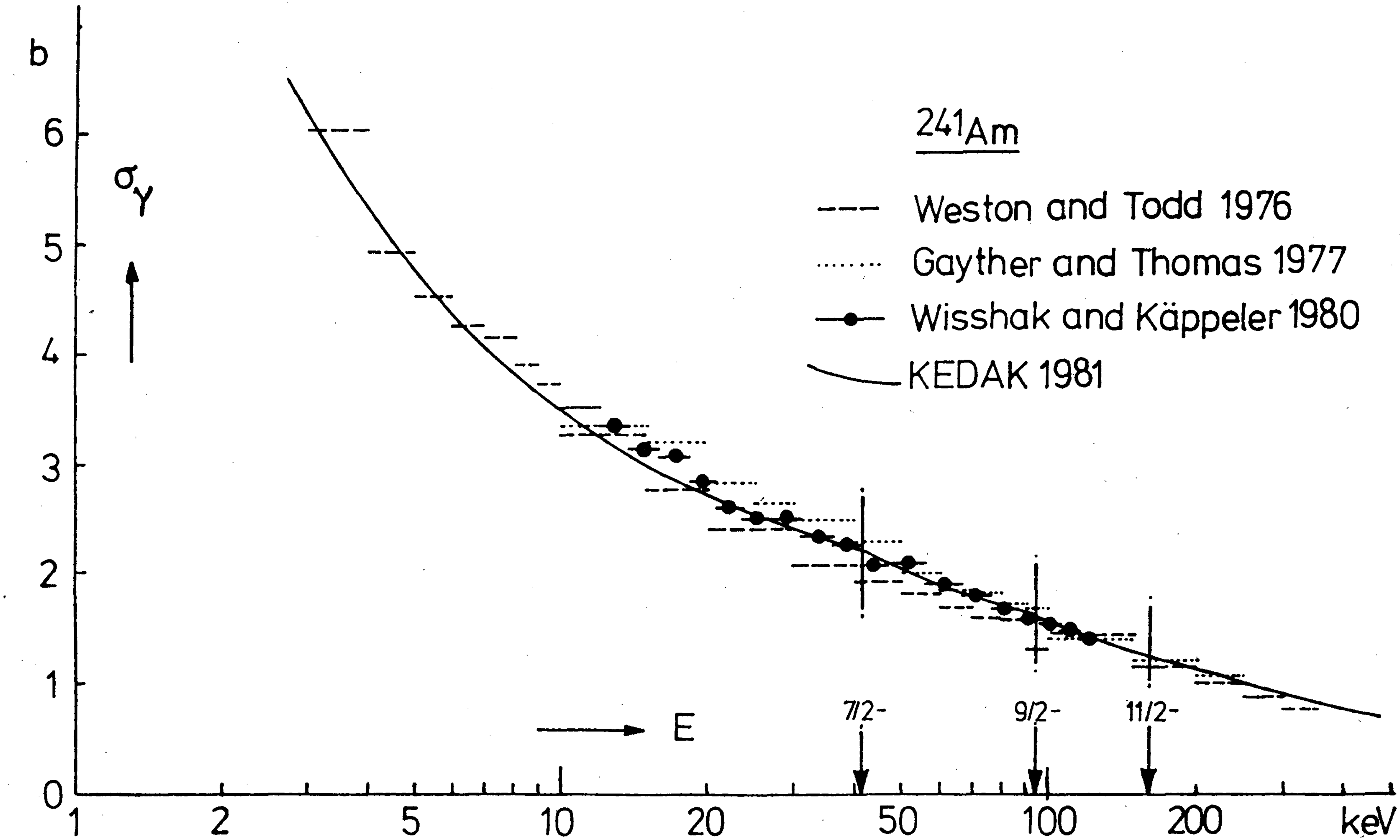

Fig. 1 - Measured and calculated capture cross sections for ^{241}Am+n in the unresolved resonance region. The first three inelastic thresholds, where the level-statistically calculated KEDAK curve is discontinuous, are indicated by arrows and by the spins and parities of the residual excited levels.

1.2 Level density estimation with account of unrecognised multiplets

F.H. Fröhner

The program STARA [1] was originally checked carefully against Monte Carlo sampled resonance ladders. It was therefore unexpected that in the benchmark exercise initiated by P. Ribon and supported by NEA [2] strength functions were estimated correctly but average level spacings were overestimated systematically (by 7.5% on average in those cases were the code should work with high accuracy). Closer inspection showed that this bias was caused by unrecognised multiplets, a possibility which had not been simulated in the Monte Carlo tests. In order to remove the bias the estimation problem was reformulated, with the width distribution

$$p(G)dG \propto (a_1 p_1(G) + a_2 p_2(G) + \ldots)dG, \quad 0 < G \equiv g\Gamma_n^0 < \infty$$

instead of the pure Porter-Thomas distribution $p_1(G)$, where a_1, a_2,... are the fractions of observed peaks which are singlets, doublets ..., and $p_2(G)$ is a χ^2 distribution with 2 degrees of freedom etc. This corresponds to the (approximately valid) assumption that the apparent neutron width of a multiplet peak as obtained from transmission data is equal to the sum of the component neutron widths. The code was modified accordingly and is being tested.

References

[1] F.H. Fröhner, Proc. Spec. Meeting on Neutron Cross Sections of Fission Product Nuclei, Bologna 1979, p. 145; F.H. Fröhner, KfK 2669, Karlsruhe (1978), pp. 90-92

[2] P. Ribon, NEANDC (E) 213-AL First Part (1980);
P. Ribon and P. Johnston, NEANDC (E) 213-AL Second Part (1980)

INSTITUT FÜR CHEMIE (1): NUKLEARCHEMIE
KERNFORSCHUNGSANLAGE JÜLICH

1. Neutron Data

1.1 Study of (n,t) and (n,^{3}He) Reactions

S.M. Qaim, G. Stöcklin, R. Wölfle

In continuation of earlier radiochemical studies on fast-neutron induced trinucleon emission reactions, the (n,t) reactions were investigated by vacuum extraction and gas phase counting of tritium. Cross sections were measured for the target nuclides ^{27}Al, ^{56}Fe, ^{59}Co and ^{93}Nb irradiated with 30 MeV d(Be)-break up neutrons [1]. The (n,^{3}He) cross sections were measured by the activation technique for ^{51}V and ^{53}Cr. Since our earlier mass spectrometric studies have shown that the emission of a ^{3}He-particle is favoured over the emission of (p2n), the activation data give the true (n,^{3}He) cross sections. The results for both (n,t) and (n,^{3}He) reactions are given in Table I.

Similar to the method described earlier [2], (n,t) and (n,^{3}He) cross sections were calculated by the Hauser-Feshbach method using a unified set of optical model parameters. Calculations were performed in steps of 1 MeV for incident neutron energies between 10 and 30 MeV. Taking into account the spectral distribution of the 30 MeV d(Be)-break up neutrons, the spectrum averaged theoretical (n,t) and (n,^{3}He) cross sections were deduced. These data are also given in Table I.

A comparison of the experimental and theoretical data suggests that the (n,t) reaction on ^{27}Al proceeds mainly via compound nucleus formation; with increasing target mass, however, the contribution of statistical processes decreases. In the case of (n,^{3}He) reactions the statistical processes contribute only little to the emission of ^{3}He-particles.

In order to investigate the mechanism of triton emission from excited nuclei work on the measurement of excitation functions of (n,t) reactions in the energy region of 15 to 20 MeV, initiated in collaboration with the CBNM Geel, was continued. First measurements on ^{27}Al and ^{93}Nb show that the (n,t) cross section increases sharply with the incident neutron energy. The excitation function of the (n,t) reaction on ^{27}Al can be described well by the Hauser-Feshbach calculations; in the case of ^{93}Nb, however, the calculated cross-section values are by an order of magnitude smaller than the experimental data.

Table I. Measured integral cross-section data and theoretically calculated data for some (n,t) and (n,^{3}He) reactions induced by 30 MeV d(Be)-break up neutrons

Nuclear reaction	$\sigma_{exp.}$ (mb)	$\sigma_{theor.}$ (mb)
$^{27}Al(n,t)^{25}Mg$	1.51	1.50
$^{56}Fe(n,t)^{54}Mn$	0.41	0.07
$^{59}Co(n,t)^{57}Fe$	0.49	0.12
$^{93}Nb(n,t)^{91}Zr$	0.49	0.03
$^{51}V(n,^3He)^{49}Sc$	0.25	0.001
$^{53}Cr(n,^3He)^{51}Ti$	0.26	0.003

1.2 Investigation of [(n,d)+(n,n'p)+(n,pn)] Reactions

S.M. Qaim, R. Wölfle

(Relevant to request identification numbers: 781024, 781025, 781027, 781053, 781057, 781058, 781104, 781106, 781108, 781215, 782078)

Cross sections for [(n,d)+(n,n'p)+(n,pn)] reactions were measured at 14.7±0.3 MeV for ^{44}Ca, ^{49}Ti, ^{50}Cr, $^{67,68}Zn$, ^{92}Zr and $^{97,98}Mo$ by the activation technique using enriched isotopes as target materials, modern radiochemical separations and high-resolution counting methods [3]. Some systematic trends observed in the cross-section data are shown in Fig. 1. Similar to other (n,charged particle) reactions the [(n,d)+(n,n'p)+(n,pn)] reaction cross section decreases as a function of (N-Z)/A; the data, however, fall on two curves, one for nuclei with neutron separation energies (S_n) higher than the proton separation energies (S_p) and the other for nuclei with $S_n < S_p$.

The cross-section data are plotted in Fig. 2 against the relative separation energy difference parameter, $(S_p-S_n)/[(N-Z)/A]$. In addition to our activation data adjusted values from charged particle measurements carried out at Livermore are also shown. The strong dependence of the cross section on the negative values of the energy parameter shows that, of the three processes involved, viz. (n,d), (n,n'p) and (n,pn), the

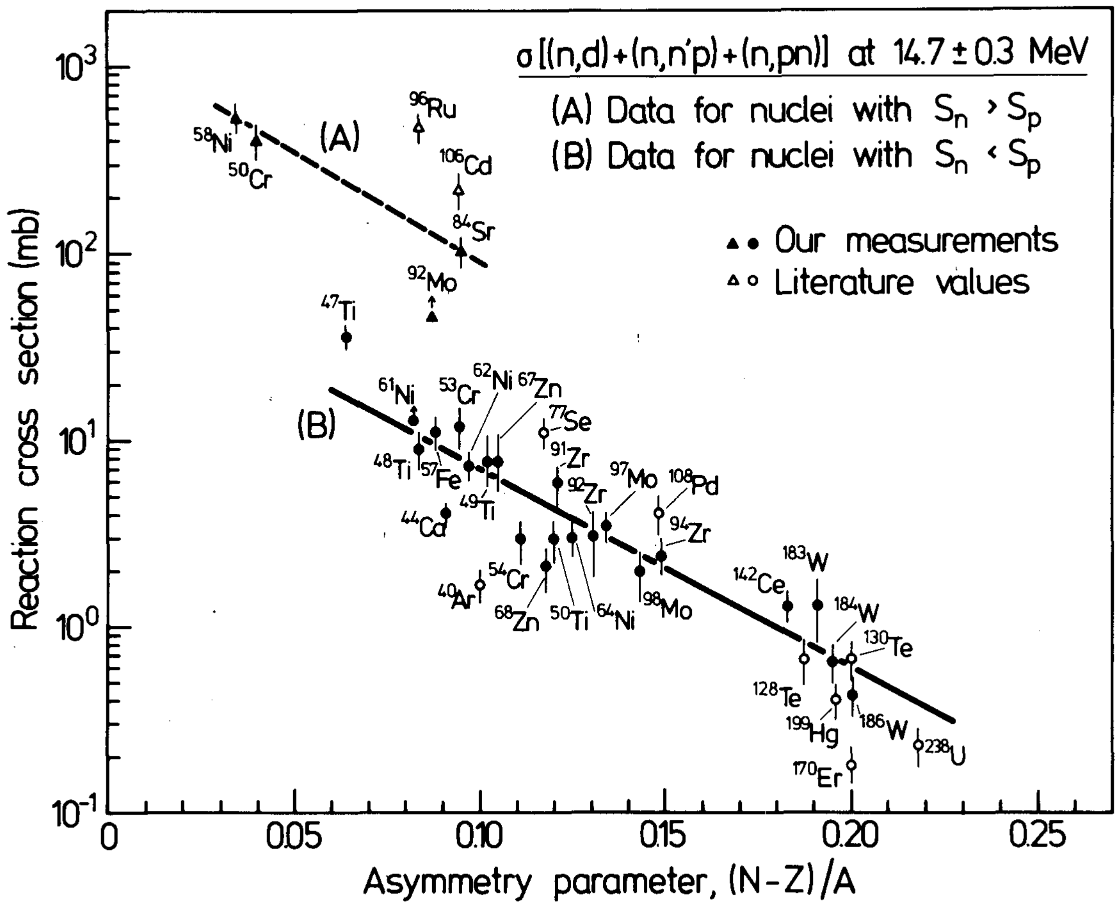

Fig. 1 Systematics of [(n,d)+(n,n'p)+(n,pn)] reaction activation cross sections induced by 14.7±0.3 MeV neutrons.

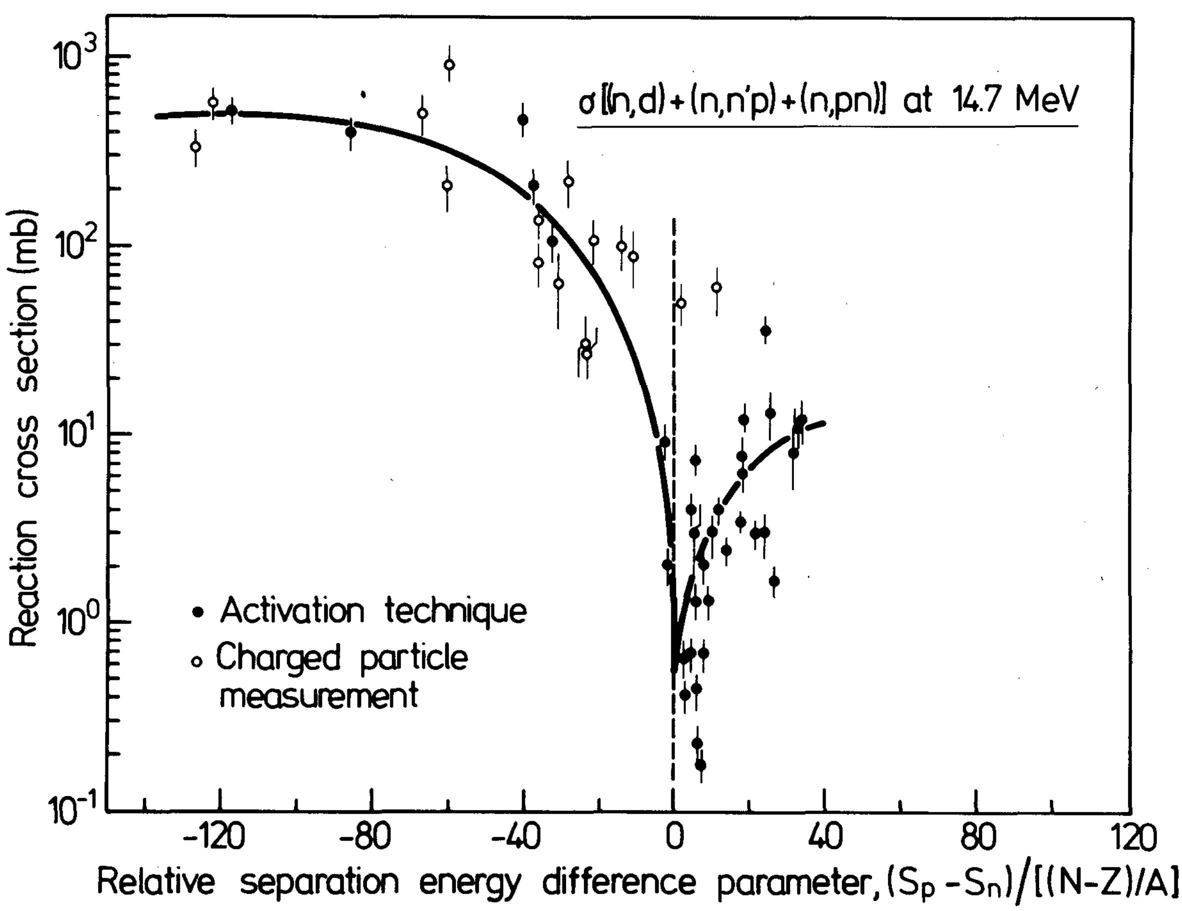

Fig. 2 σ[(n,d)+(n,n'p)+(n,pn)] as a function of the relative separation energy difference parameter.

(n,n'p) process is the dominating mode of decay. For nuclei with $S_n < S_p$ the relative energy parameter is positive and the cross section increases with the increasing energy parameter. For all those nuclei the cross sections are relatively small and have been advantageously measured by the activation technique.

Measurements of [(n,d)+(n,n'p)+(n,pn)] reaction cross sections were also carried out with 30 MeV d(Be)-break up neutrons [1,4]. The cross sections are in general higher than those at 14.7 MeV.

1.3 Measurement of Excitation Function of $^{7}Li(n,n't)^{4}He$ Reaction

H. Liskien*, S.M. Qaim, R. Wölfle

(Relevant to request identification numbers: 724007, 724008, 732004, 762058, 762246, 781159, 792105)

With a view to clearing discrepancies in the $^{7}Li(n,n't)^{4}He$ reaction cross sections, a measurement programme over the neutron energy range of 4 to 10 MeV has been started. Highly enriched ^{7}Li samples are irradiated and the formed tritium is separated and counted in the gas phase. The results obtained so far indicate that the excitation function is about 15% lower than the ENDF B IV curve. Further measurements are in progress.

2. Charged Particle Data for Radioisotope Production

H. Backhausen, He Youfeng+, S.M. Qaim, G. Stöcklin, R. Weinreich

In continuation of our studies [5,6] on the production of short-lived β^{+} emitting radionuclides, cross-section measurements were performed for nuclear reactions leading to the formation of ^{18}F [7] and ^{77}Kr [8].

^{18}F ($T_{1/2}$ = 110 min) can be produced via the reaction $^{20}Ne(^{3}He,\alpha p)^{18}F$, the excitation function of which is well known. Additionally, the process $^{20}Ne(^{3}He,\alpha n)^{18}Ne \xrightarrow[1.67\ sec]{\beta^{+}} {}^{18}F$ can also contribute. Due to the short half-life of ^{18}Ne this route had not been investigated. We developed a method for fast removal of ^{18}Ne. Stacked gas targets were irradiated and a flow

---

* CBNM, Geel, Belgium

+ On leave from Institute of Atomic Energy, Academia Sinica, Peking, People's Republic of China absorption technique was applied using alumina chromatographic columns to trap the decay produced ^{18}F. The directly formed ^{18}F was adsorbed in the first column, and that formed via the decay of ^{18}Ne, while passing through the columns, was adsorbed in all the columns. Through measurement of the daughter ^{18}F activity it was possible to determine the cross sections for the formation of ^{18}Ne. The results are shown in Fig. 3. Evidently the contribution of the $^{20}Ne(^{3}He,\alpha n)^{18}Ne \xrightarrow[1.67\ sec]{\beta^+} {}^{18}F$ process to the total formation of ^{18}F is small. However, this process may lead to some interesting decay produced ^{18}F-species. Those species may find use in labelling of biomolecules.

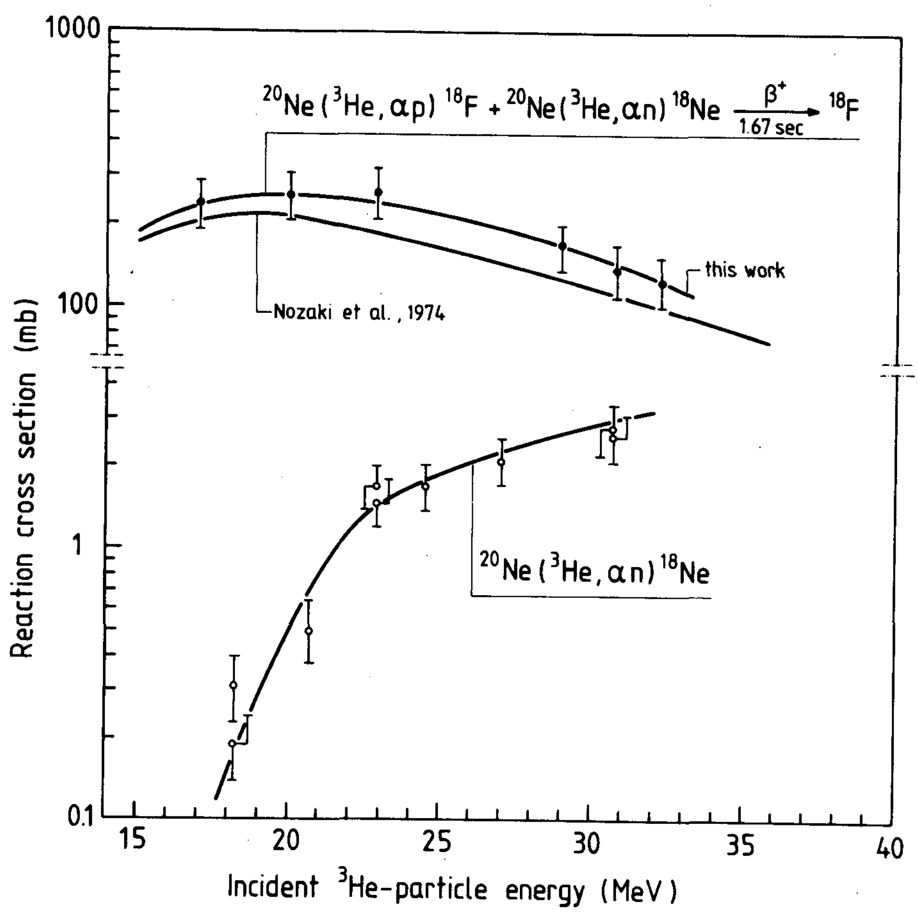

Fig. 3 Excitation functions for the formation of ^{18}F via $^{20}Ne(^{3}He,\alpha p)^{18}F$ and $^{20}Ne(^{3}He,\alpha n)^{18}Ne \xrightarrow[1.67\ sec]{\beta^+} {}^{18}F$ processes.

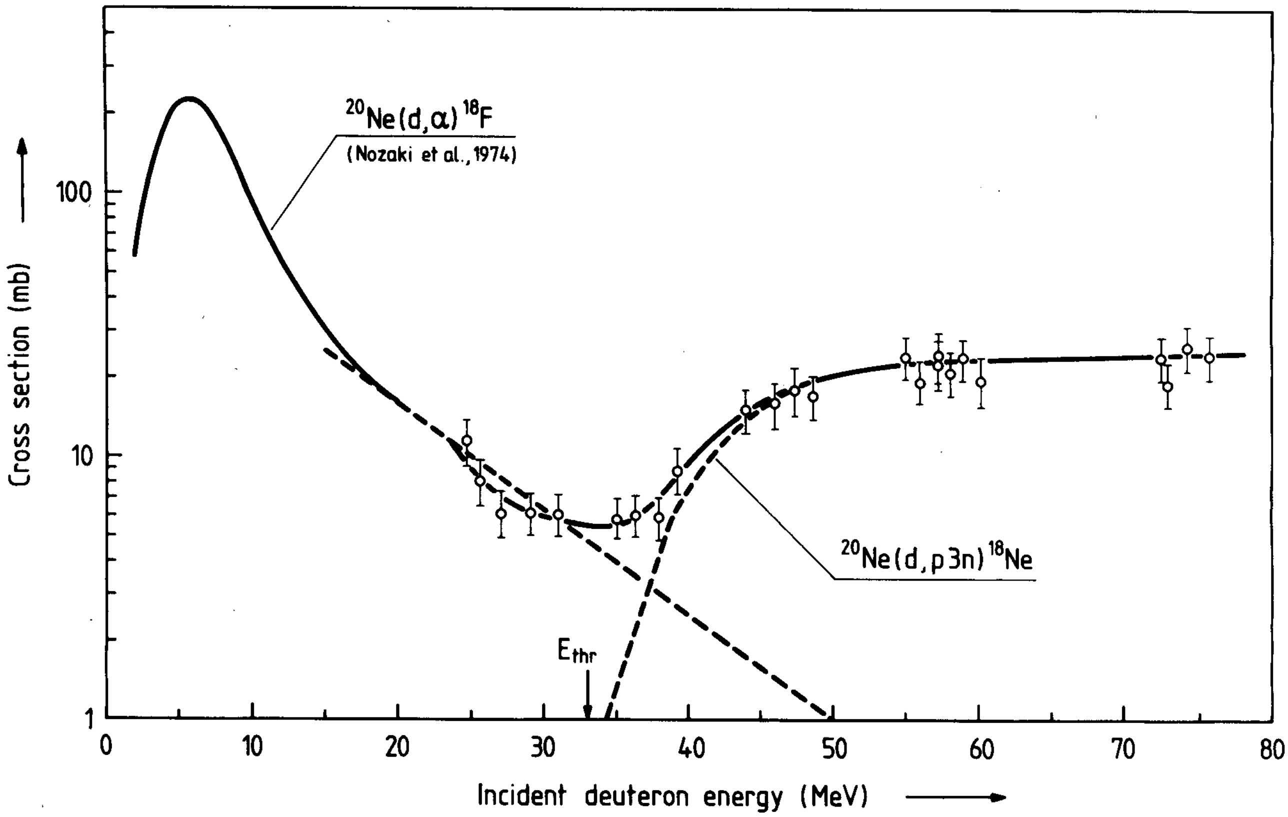

Fig. 4 Excitation functions for deuteron induced nuclear reactions on neon. The (d,p3n)-reaction product contains contributions from the (d,d2n)- and (d,tn)-reactions.

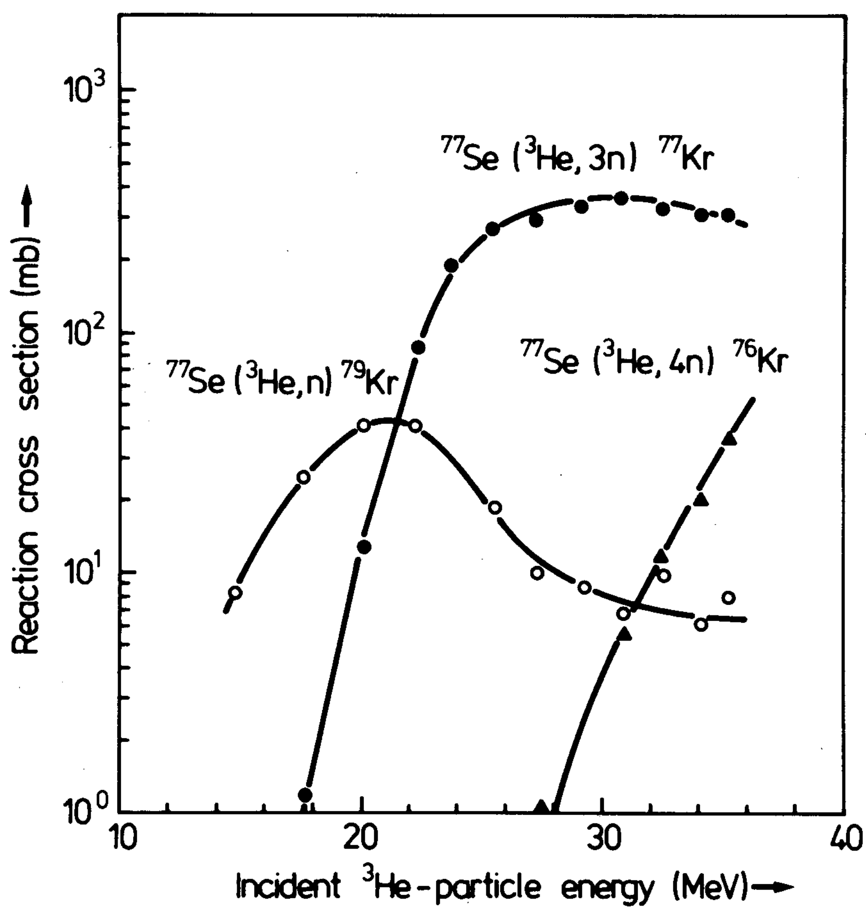

Fig. 5 Excitation functions for the formation of ^{76,77,79}Kr in ^{3}He-particle induced nuclear reactions on ^{77}Se.

Another method for the production of ^{18}F is via deuteron induced reactions on ^{20}Ne. Here also the excitation function for the direct formation of ^{18}F was known but not that for its formation via the ^{18}Ne precursor. In this case conventional static target technique was used. The results are shown in Fig. 4. In the high energy region the cross section for the process $^{20}Ne(d,x)^{18}Ne \xrightarrow[1.67\ sec]{\beta^+} {}^{18}F$ is not too small and thus at high energy machines this reaction can be used for the production of ^{18}F. For a target thickness corresponding to $E_d = 65 \rightarrow 60$ MeV, ^{18}F yield of 5 mCi/µAh can be obtained.

^{77}Kr ($T_{1/2}$ = 72 min) can be produced via p or d induced reactions on bromine. The product is, however, contaminated with ^{79}Kr. We investigated the ^{3}He-induced reactions on enriched ^{76}Se and ^{77}Se. Excitation functions were measured by the 'stacked-pellet technique'. The results for ^{3}He-induced reactions on ^{77}Se are given in Fig. 5. Through integration of the excitation functions it was found that for a target thickness corresponding to $E_{^3He} = 36 \rightarrow 15$ MeV, ^{77}Kr yields of 11.5 mCi/µAh can be obtained. The levels of impurities due to ^{79}Kr and ^{76}Kr at EOB amount to 0.35% and 0.36%, respectively.

References

[1] S.M. Qaim, S. Khatun, R. Wölfle, Integral cross-section measurements on (n,x) reactions induced by 30 MeV d(Be)-break-up neutrons on FRT wall and structural materials, Proc.Symp. on Neutron Cross Sections from 10 to 50 MeV, Brookhaven (May 1980), BNL-NCS-51245, Vol. II (1980) 539

[2] S.M. Qaim, H.V. Klapdor, H. Reiss, Statistical model analysis of cross sections of (n,t) and (n,^{3}He) reactions induced by 14.6 MeV neutrons on target nuclei with A = 27 to 59, Phys.Rev. C22 (1980) 1371

[3] S.M. Qaim, (n,d), (n,n'p) and (n,pn) reactions at 14.7 MeV, submitted to Phys.Rev.C.

[4] S.M. Qaim, R. Wölfle, G. Stöcklin, Radiochemical studies of fast neutron induced reactions at KFA Jülich, Proc. 5th National Soviet Conference on Neutron Physics, Kiev, 15-19 September 1980, in press

[5] R. Weinreich, Z.B. Alfassi, G. Blessing, G. Stöcklin, Short-lived neutron deficient bromine isotopes for applications in nuclear medicine, Proc. 17th Intern.Annual Meeting, Soc.Nucl.Med., Innsbruck 1979, Nuklearmedizin: Suppl. 17 (1980) 202

[6] G. Comparetto, S.M. Qaim, A comparative study of the production of short-lived neutron deficient isotopes $^{94,95,97}Ru$ in α- and ^{3}He-particle induced nuclear reactions on natural molybdenum, Radiochimica Acta 27 (1980) 177

[7] H. Backhausen, G. Stöcklin, R. Weinreich, Formation of ^{18}F via its ^{18}Ne precursor: Excitation functions of the reactions $^{20}Ne(d,x)^{18}Ne$ and $^{20}Ne(^{3}He,\alpha n)^{18}Ne$, Radiochimica Acta, in press

[8] He Youfeng, S.M. Qaim, G. Stöcklin, Excitation functions for ^{3}He-particle induced nuclear reactions on ^{76}Se, ^{77}Se and ^{nat}Se: Possibilities of production of ^{77}Kr, submitted to Int.J.appl.Radiat. Isotopes

I. INSTITUT FÜR EXPERIMENTALPHYSIK
UNIVERSITÄT HAMBURG

1. Continuous Proton and α Particle Spectra from α + ^{59}Co, ^{60}Ni

R. Scherwinski, J. Friese, C. Heidorn, W. Scobel

Charged particle emission from reactions induced on ^{59}Co (^{60}Ni) with α-particles of E_{α} = 28.5 MeV (32 MeV) from the Hamburg Isochronous Cyclotron has been studied with solid state detector telescopes for reaction angles ranging from $\Theta_{lab} = 15^{\circ}$ to 160°. These data supplement the preceding (α,xn)-time-of-flight experiment [1] for the same target nuclei and energies.

The resulting double differential cross sections, integrated over ΔE = 2.2 MeV intervals, are shown in Figs. 1,2. They reveal the influence of non-equilibrium contributions at foreward angles and high energies, respectively; so do the energy spectra shown for some selected angles.

In order to describe the angle integrated α-particle spectra we have applied a Hauser-Feshbach calculation in combination with the quasi free scattering model [2] for the preequilibrium (PE) component. The parameters of the PE calculation are those that describe our (p,α)-results for 26.5 MeV protons on $^{58-64}$Ni, ^{63,65}Cu best [3]; in particular a preformation probability Φ = 0.1 and a Fermi energy of ε_F = 6 MeV per nucleon correlated to an α particle has been adopted from the (p,α) analysis. The agreement with the high energy continuum (Fig. 2) underlines that the model allows a consistent description of (p,p'), (p,α), (α,p) and (α,α') PE-emission; the deviation from the experimental results is smaller than that obtained between two Hauser-Feshbach results for the equilibrium component that differ in parameters of level density (a) and g.s. energy shift (Δ) for the back shifted Fermi gas model.

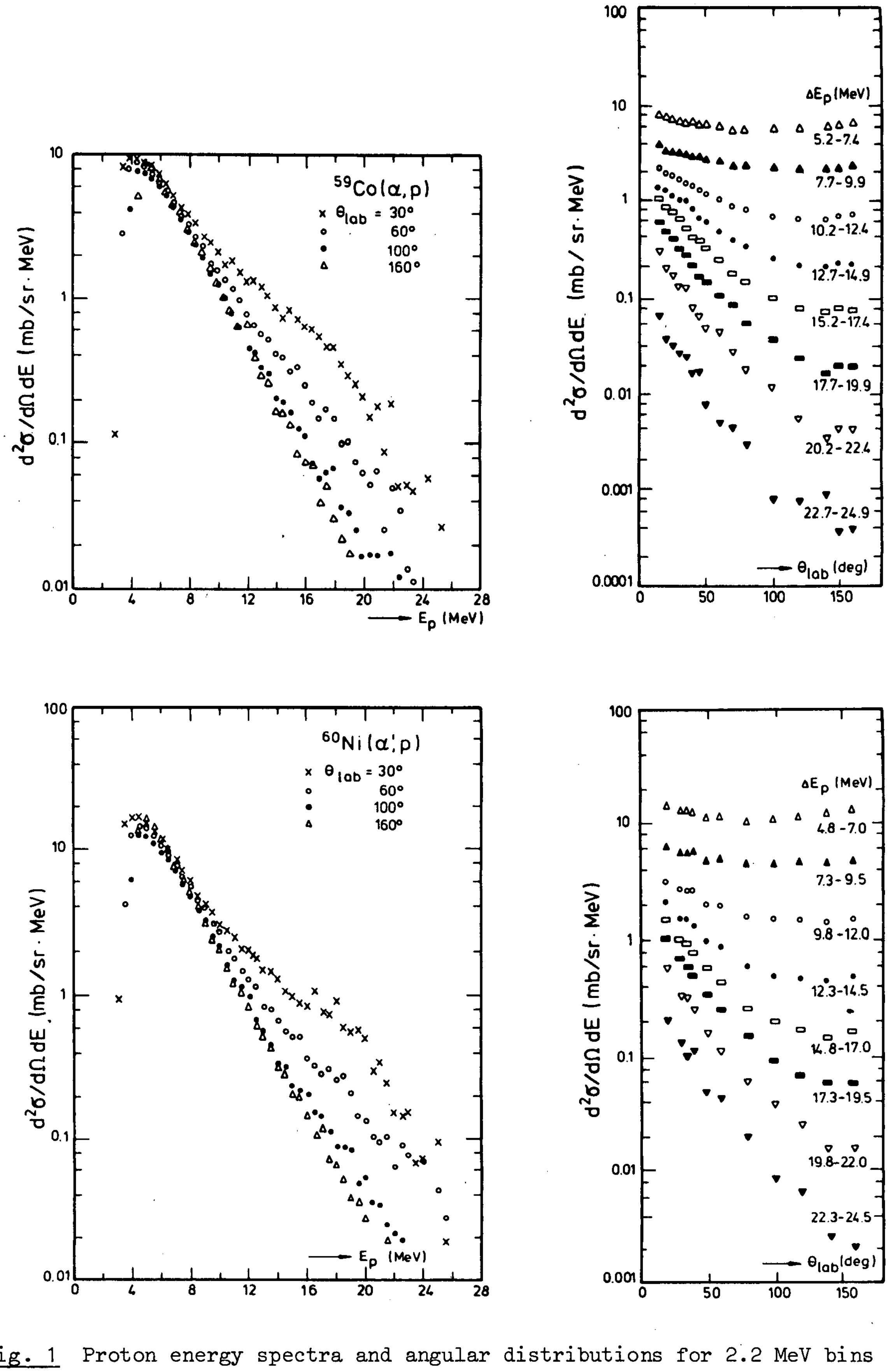

Fig. 1 Proton energy spectra and angular distributions for 2.2 MeV bins

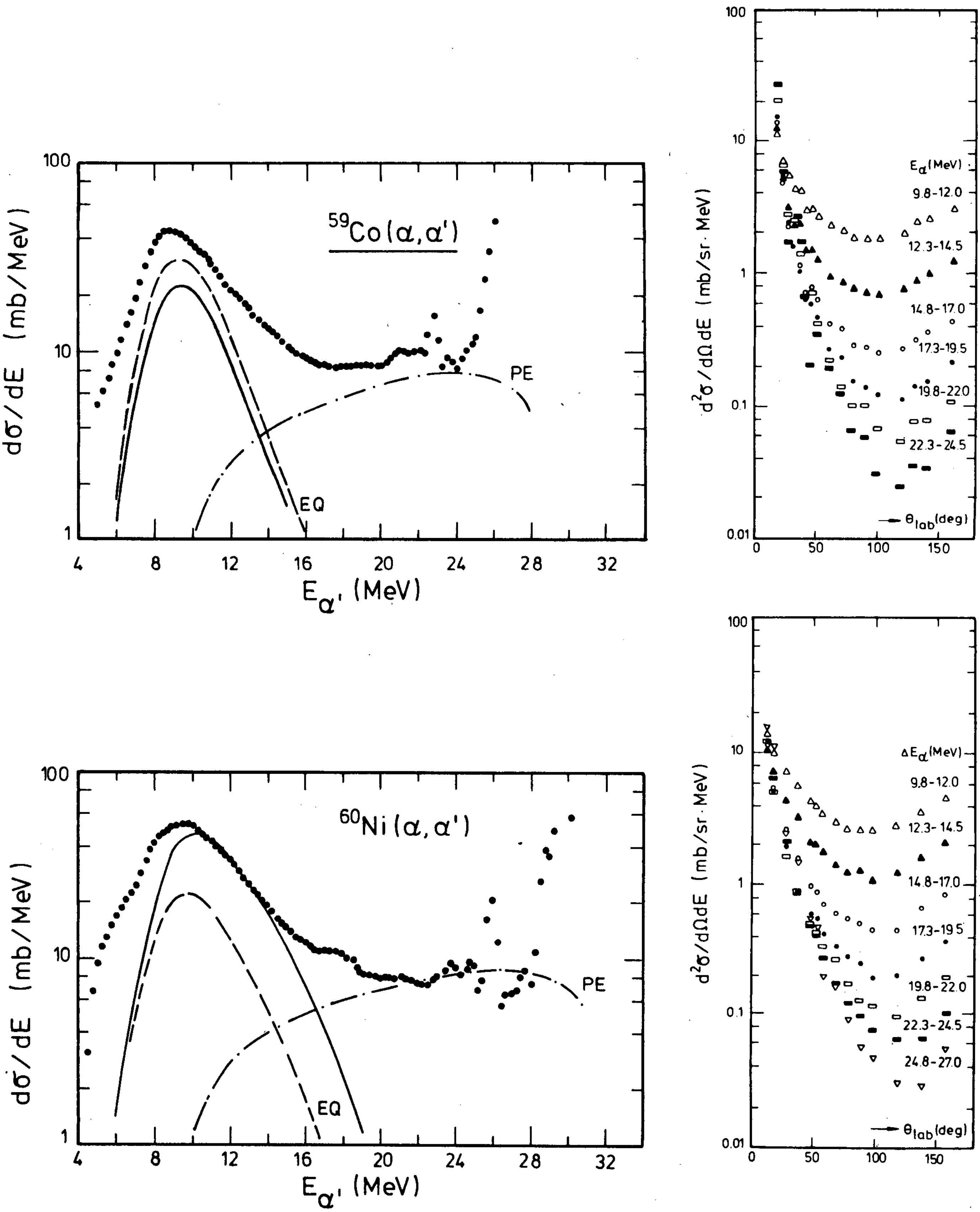

Fig. 2 Angular distributions and angle integrated α particle energy spectra, compared with PE model [2] and Hauser-Feshbach calculations. Dashed (solid) lines: parameters from ref. [4] ([3]).

2. Preequilibrium Decay of $^{63}Cu^*$, $^{64}Zn^*$ by Nucleon Emission

R. Scherwinski, A. Alevra*, R. Langkau, W. Scobel, R. Wien

The angle integrated energy spectra of protons from (α,xp) reactions for targets in the mass region $A \approx 60$ and energies $E_\alpha \approx 20$-24 MeV indicate [5], that for even-even targets (like ^{60}Ni) the PE contributions correspond to an initial $n_o=4$ exciton configuration with 2 neutrons, 2 protons and no holes (2n, 2p, 0h), whereas for odd mass targets (like ^{59}Co) an $n_o=5$ configuration (2n, 3p, 0h) seems to be favoured. The interpretation in terms of the unpaired nucleon plus 4 α-particle nucleons is obvious.

In contrast to this result, the neutron energy spectra of the (α,xn) reactions with 28.5 and 32 MeV projectiles on both, ^{60}Ni and ^{59}Co, showed a preference of $n_o=4$ if analyzed [1] with a combination of Ewing-Weißkopf and Hybrid model.
The puzzle is solved if a Hauser-Feshbach or Ewing-Weißkopf (EQ) plus hybrid (PE) model calculation with shifted ground state is applied instead. Fig. 3 shows the results for the (α,xn) data mentioned and the (α,xp) spectra of the preceding contribution. For <u>all</u> level densities (EQ and PE) a shift of the ground state by $\Delta_{uu} = -2.0$ MeV, $\Delta_{ug} = \Delta_{gu} = -0.7$ MeV and $\Delta_{gg} = +0.6$ MeV has been taken into account for odd-odd, odd mass and even-even nuclei, respectively [4]. Due to the back shift correction a consistent description of the PE neutron <u>and</u> proton channel is obtained with $n_o=4$ for ^{60}Ni + α and $n_o=5$ for ^{59}Co. The importance of this shift is best seen for the only reaction with an odd-odd residual nucleus (where the correction is greatest), namely ^{59}Co(α,n)^{62}Cu. Fig. 3 shows that one ends with the inconsistent result $n_o=4$ if the shift is not applied.

<u>Fig. 3</u> Angle integrated nucleon energy spectra. Calculations:

a) Hybrid model for internal transition rates λ_+^{NN}/k with $k = 1.5$ and initial configuration $n_o=4$ (2,2,0) and ground state shift Δ (dashed line).

b) Same as a), but for $n_o=5$ (2,3,0).

c) Ewing-Weißkopf model with $a = \frac{A}{8}$ MeV^{-1} and shifted ground state (long dashed).

d) Hauser-Feshbach with parameters of [4] (short dashed).

e) Solid line: Sum of c) and b) or a), respectively.

f) For ^{59}Co(α,xn), calculations a) and b) without shift Δ are shown as dotted lines.

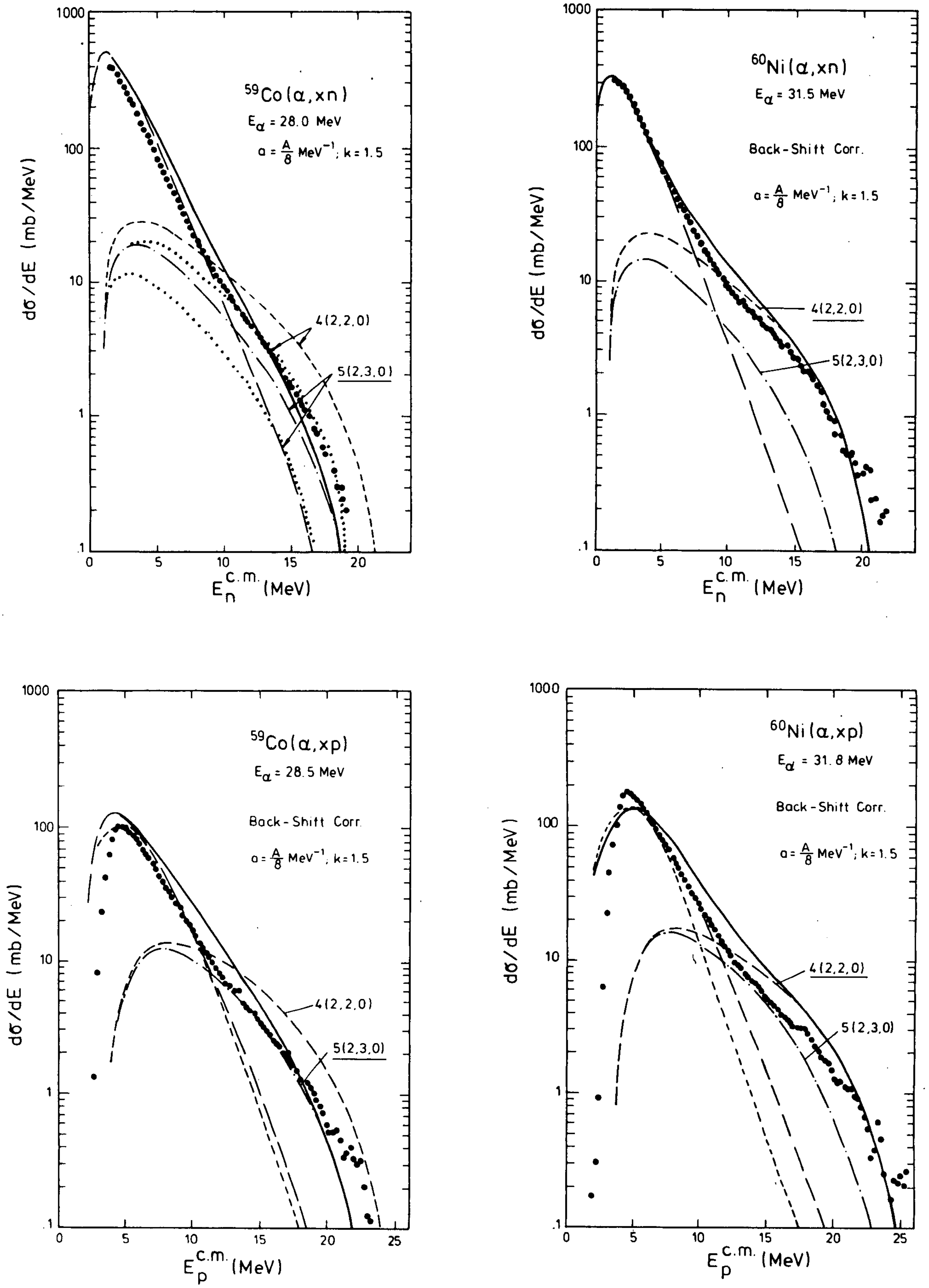

$^{59}Co(\alpha,xn)$
E_α = 28.0 MeV
$a = \frac{A}{8}$ MeV^{-1}; k = 1.5
4(2,2,0)
5(2,3,0)
dσ/dE (mb/MeV)
$E_n^{c.m.}$ (MeV)
$^{60}Ni(\alpha,xn)$
E_α = 31.5 MeV
Back-Shift Corr.
$a = \frac{A}{8}$ MeV^{-1}; k = 1.5
4(2,2,0)
5(2,3,0)
$^{59}Co(\alpha,xp)$
E_α = 28.5 MeV
Back-Shift Corr.
$a = \frac{A}{8}$ MeV^{-1}; k = 1.5
4(2,2,0)
5(2,3,0)
$E_p^{c.m.}$ (MeV)
$^{60}Ni(\alpha,xp)$
E_α = 31.8 MeV
Back-Shift Corr.
$a = \frac{A}{8}$ MeV^{-1}; k = 1.5
4(2,2,0)
5(2,3,0)

Fig. 3

3. Angular Distributions in $^{63}Cu^*$ and $^{64}Zn^*$ PE Decay by n,p,α Emission

A. Alevra*, R. Langkau, R. Scherwinski, W. Scobel

The exciton model recently [6,7] has been extended such that particle unbound states are distinguished during equilibration from bound states. This is then the clue to a separation into foreward peaked multi-step direct (MSD) and multi-step compound (MSC) preequilibrium contributions in the spirit of [8]. The shapes of the angular distributions are in this model described in terms of Legendre polynomials $P_\ell(\cos\Theta)$

$$\frac{d^2\sigma}{d\Omega d\varepsilon}(a,b) = a_o^{MSD} \sum_{\ell=0}^{\ell_{max}} b_\ell(\varepsilon)P_\ell + a_o^{MSC} \sum_{\substack{\ell=0 \\ \Delta\ell=2}}^{\ell_{max}} b_\ell(\varepsilon)P_\ell \qquad (1)$$

where $a_o^{MSD} + a_o^{MSC} = \frac{1}{4\pi}\frac{d\sigma}{d\varepsilon}$ and the polynomial coefficients $b_\ell(\varepsilon)$ are derived phenomenologically from existing experimental data. This semi-empirical model predicts $b_\ell(\varepsilon)$ to be (i) <u>not</u> dependent on the projectile energy; (ii) <u>not</u> sensitive to the target mass; (iii) <u>not</u> dependent on the type of the outgoing particle b, only on its energy ε; (iv) only slightly (if at all) dependent on the type of projectile.

The (α,xn), (α,xp) and (α,xα) data presented here and in [1] in combination with the corresponding results [3] for the proton induced reactions are particularly suited to test the predictions (iii) and (iv). For simplification we have assumed 100% MSC (MSD) contributions at low (high) ejectile energies.

Examples for angular distributions of protons and α particles are shown in Figs. 4 and 5. The low energy protons (E_p = 5-6 MeV) are in agreement with the MSC prediction, whereas for the low energy α-particles (10-11 MeV) the MSD contribution cannot be neglected. At high energies the calculation in spite of the 100% MSD assumption underestimates the foreward peaking for the (α,xp) and (α,xα) cases, whereas the agreement is better for the (p,xp) and (p,xα) data; our data therefore do not quantitatively support prediction (iv).

---

* Permanent address: Institutul de Fizica si Inginerie Nucleara,
Bucharest, Romania

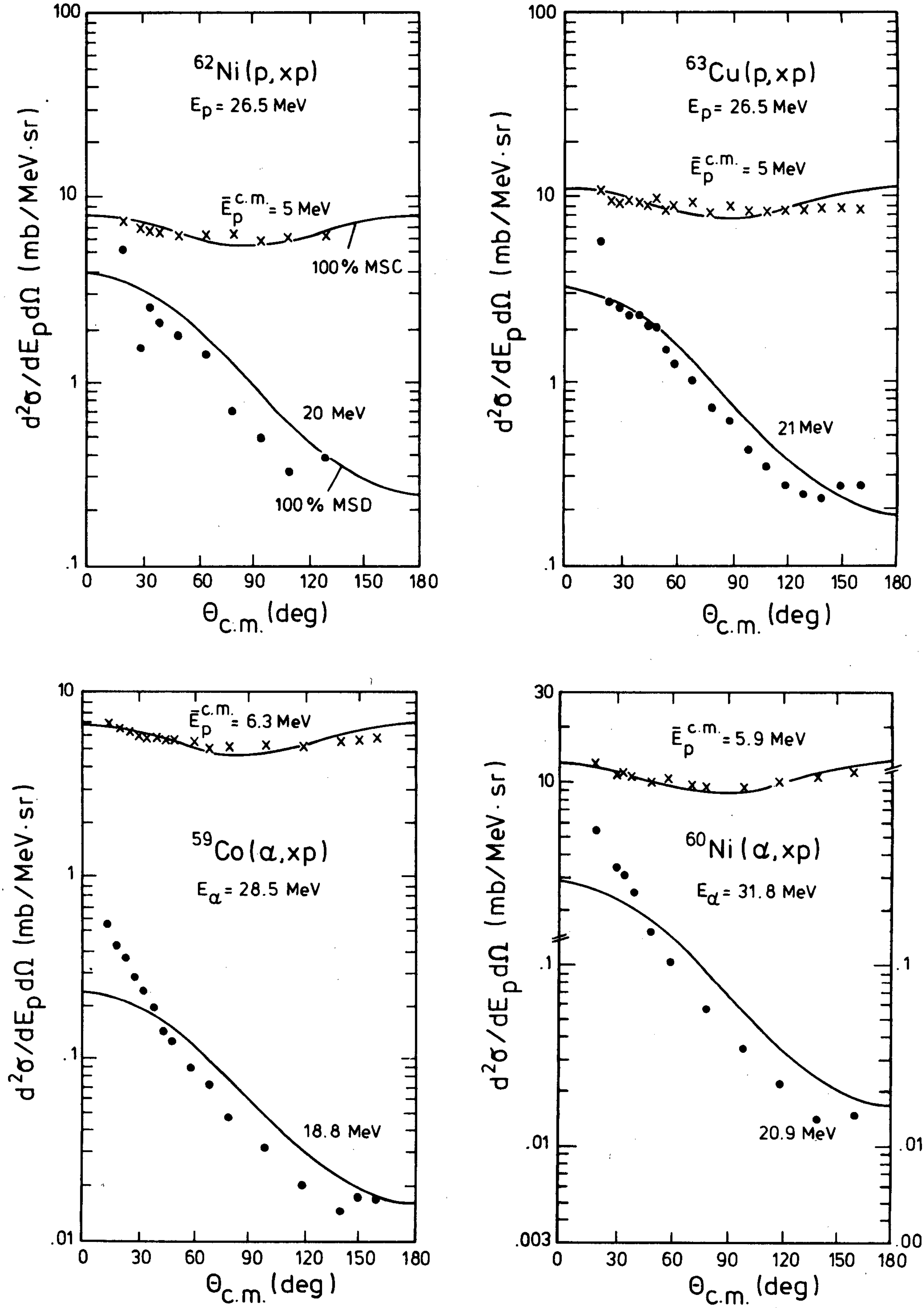

Fig. 4 Angular distributions of protons emitted during deexcitation of ^{63}Cu (E^* = 32.2 MeV) and ^{64}Zn (E^* = 33.8 MeV). Solid lines are (normalized) exciton model calculations.

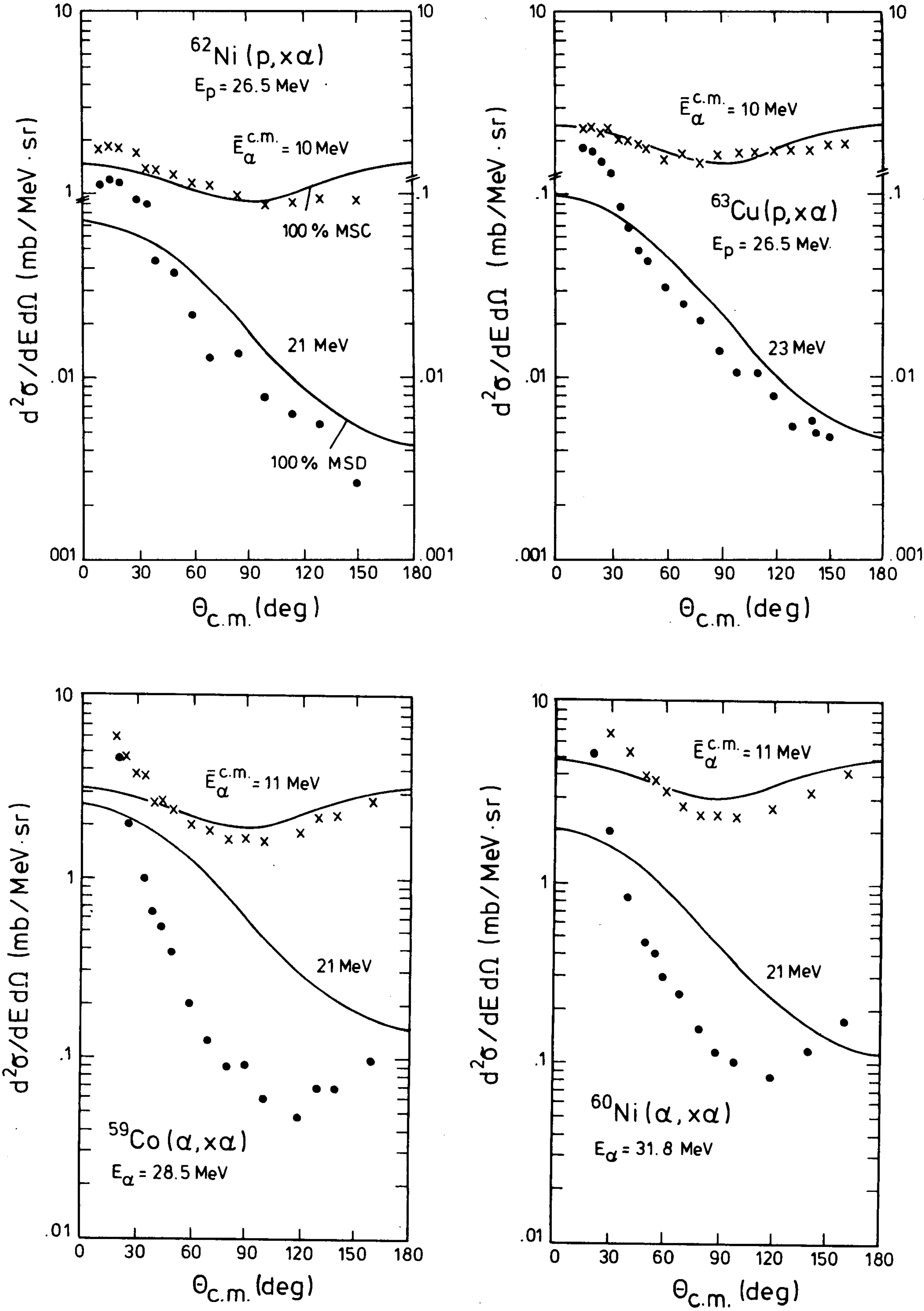

Fig. 5 Same as Fig. 4 for α-particles.

References

[1] A. Alevra, H.H. Bissem, R. Langkau, P. Plischke, W. Scobel, NEANDC(E)-202U Vol V(1979)p. 59

[2] W. Scobel, M. Blann, A. Mignerey, Nucl. Phys. A287(1977)301

[3] W. Scobel, Proc. Workshop on Reaction Models for Continuous Spectra of Light Particles (Bad Honnef, 1978), p. 65

[4] W. Dilg, W. Schantl, H. Vonach, M. Uhl, Nucl. Phys. A217(1973)269

[5] A. Alevra, M. Duma, I.R. Lucas-Koch, M.T. Magda, M.E. Nestor, Nucl. Phys. A265(1976)376

[6] C. Kalbach, F.M. Mann, Phys. Rev. C23(1981)112

[7] C. Kalbach, Phys. Rev. C23(1981)124

[8] H. Feshbach, A. Kerman, S. Koonin, Ann. Phys. 125(1980)429

INSTITUT FÜR REINE UND ANGEWANDTE KERNPHYSIK
UNIVERSITÄT KIEL , FORSCHUNGSREAKTOR GEESTHACHT

Fast-Chopper Time-of-Flight Spectrometer

H.G.Priesmeyer, U.Harz, P.Fischer

1. Flightpath calibration and energy correction of the low-energy Iridium resonances .

During the flightpath calibration experiment - using the low-energy resonances of 238 U and iridium as standards (cf. James, NBS SP 493 (1977), 319) - it was realised that the resonance energy of 191 iridium differed from the value quoted as standard, when the flight path was derived from the 238 U - resonances alone. This seems to be resonable, because the values given by James are results of very different experiments: the iridium experiment was a chopper experiment aimed at resonance parameter determination, whereas the uranium measurements were carefully designed calibration experiments. Therefore we regard it necessary to adjust the iridium data to the uranium measurements.SHAPE fits (Atta-Harvey) of our data are given in Fig.1 and 2. Detailed information about the experiment can be found in Ref.1 .

The following data were obtained:

Isotope	E_o [eV]	Γ_γ [meV]	$2g\Gamma_n^o$ [meV]
191 Ir	0.6528 ± 0.0005	72.7 ± 0.5	0.679 ± 0.011
193 Ir	1.298 ± 0.001	83.2 ± 0.8	0.80 ± 0.01

2. 99 Tc transmission below 30 eV

Final results are published in ATOMKERNENERGIE (Ref.2). Detailed information is given in Ref. 3

IKK FAST CHOPPER RUN 214

ANALYSIS RUN 214-01 /01/01
SHAPE ANALYSIS OF TRANSMISSION DATA

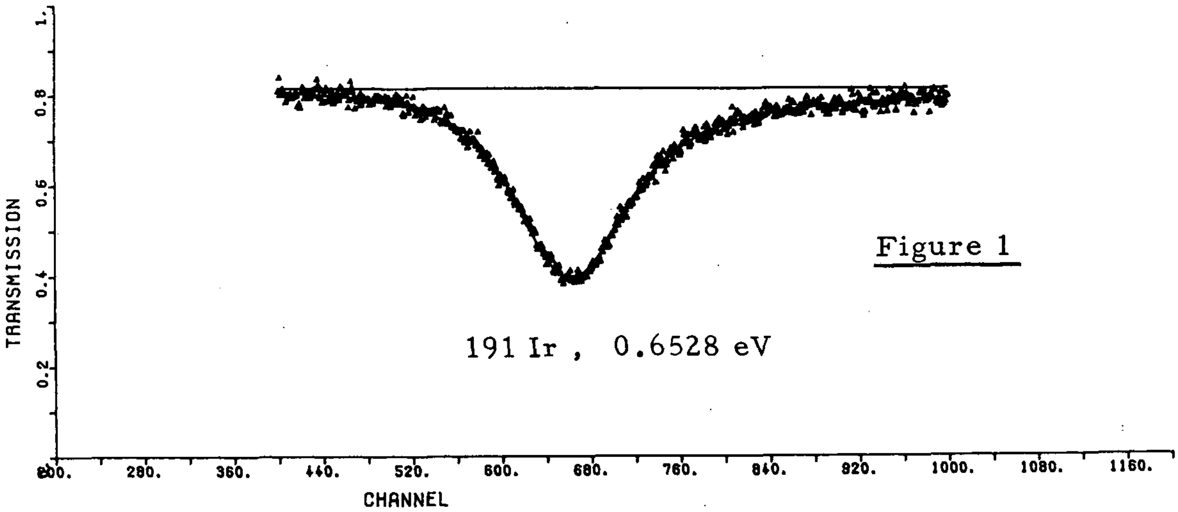

Figure 1

- THEORET. TRANSMISSION
- EXPER. TRANSMISSION
- BASELINE

IKK FAST CHOPPER RUN 214

ANALYSIS RUN 214-01 /02/01
SHAPE ANALYSIS OF TRANSMISSION DATA

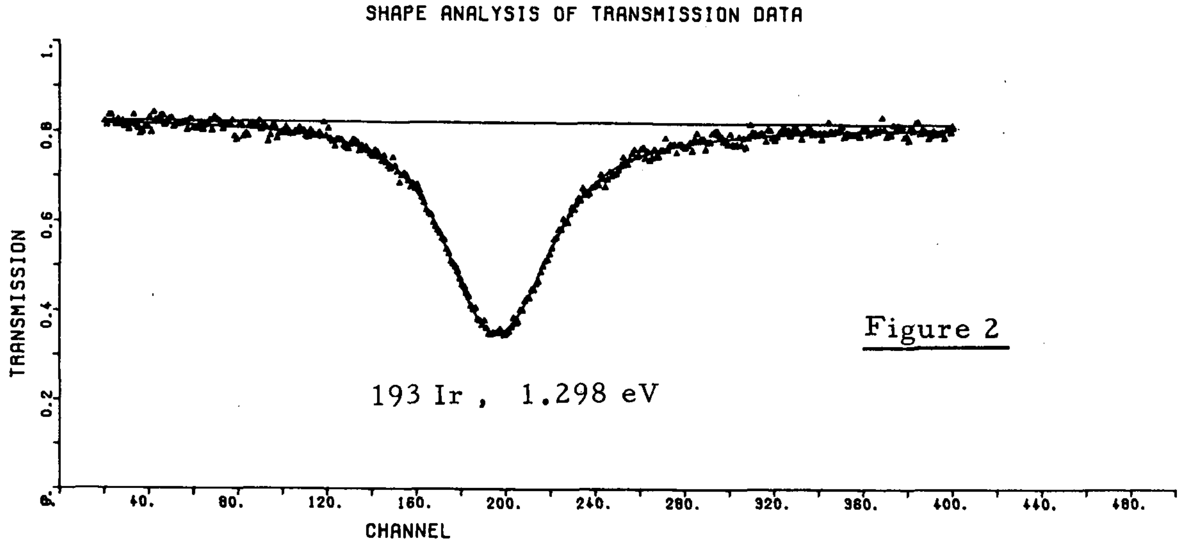

Figure 2

- THEORET. TRANSMISSION
- EXPER. TRANSMISSION
- BASELINE

SHAPE - fits of Iridium Resonances

3. Cs Fission Product Mixture

In order to identify resonances in the 600 Ci fission product sample, an experiment on stable 133 CsCl was made.

Four resonances can be attributed to radioactive Cs isotopes: at 41.895 eV, 195 eV, 423 eV and 883 eV. From figures 3 and 4, which show SHAPE - fits of measurements in the 40 eV region, a comparison can be made between the investigation made in 1969 and the one made in 1979. If the resonance at 41.895 eV were to be attributed to 137 Cs it could be seen, since 11% of that isotope have decayed.

The following parameters have been determined:

data from	Exp.No.	Γ [meV]	$2g\Gamma_n$ [meV]
1969	087	215 ± 23	32,7 ± 2
1979	209	232 ± 7	31,9 ± 0,5

The resonance belongs to 135 Cs.

The 1979 measurement had better statistics and higher energy resolution than the previous one.

The identification of the other resonances is not yet unique.

4. Publications

1. Fischer, Harz, Priesmeyer   Die Energieeichung des IKK Fast-Chopper - Die Resonanzparameter des Iridiums unterhalb 1,5 eV   GKSS 81/E/17
2. Fischer, Harz, Priesmeyer   Neutron Resonance Parameters of 99 Tc   ATKE 38(1), (1981) 63
3. Fischer   Die Resonanzparameter des Technetium 99 im Energiebereich von 4,5 bis 25 eV   GKSS 80/E/28
4. Priesmeyer   Low-energy Neutron Cross-section Measurements of Radioactive Fission Product Nuclides   NEANDC (E) 209 "L"

SHAPE ANALYSIS OF TRANSMISSION DATA

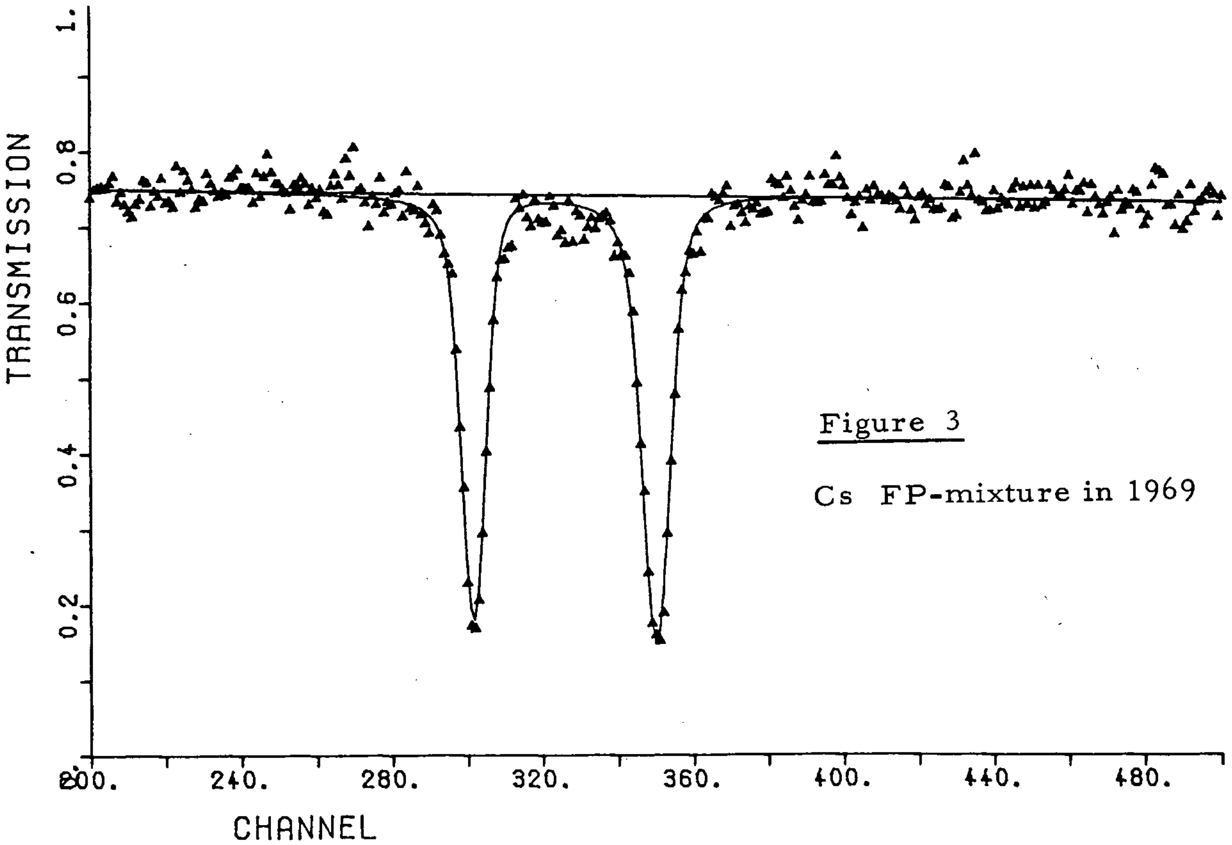

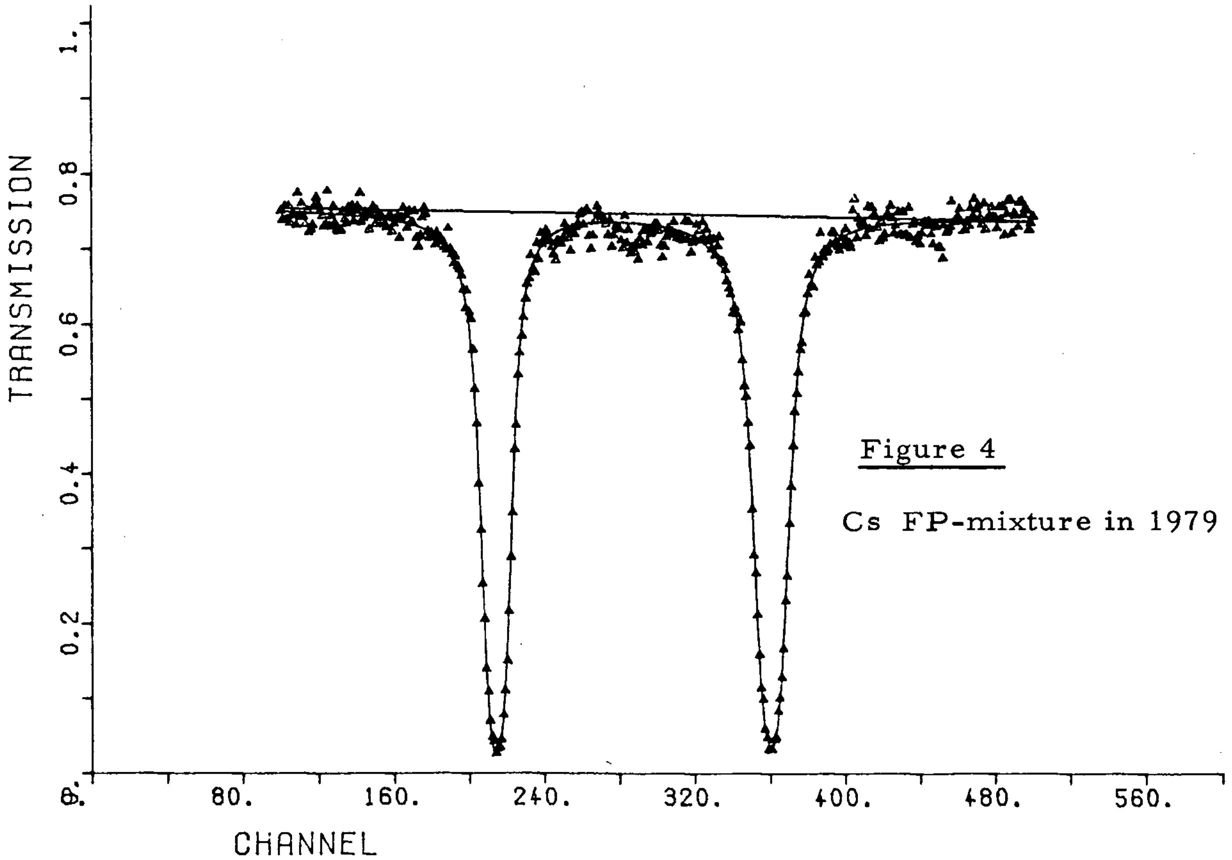

IKK FAST CHOPPER
ANALYSIS RUN

INSTITUT FÜR KERNCHEMIE
UNIVERSITÄT ZU KÖLN

Integral Excitation Functions for α-Induced Reactions on Iron and Nickel

R. Michel, G. Brinkmann and W. Herr

Thin target production cross sections can be regarded as a basis for the interpretation of cosmic ray produced radionuclides in extraterrestrial matter. Therefore, during the last years we have performed a systematic investigation of p-induced reactions with target elements $22 \leq Z \leq 28$ [1]. We now have extended our studies to α-induced reactions for the same elements [2,3]. In spite of the fact that the p/α ratio in cosmic radiation is ~10, α-induced reactions may become the dominant production modes for particular nuclides, as e.g. for ^{57}Co, ^{58}Co and ^{59}Ni. Using the stack foil technique, up to now 38 excitation functions were measured for the production of radionuclides $42 \leq A \leq 65$ from natural iron and nickel for $16 \leq E_\alpha \leq 173$ MeV [4]. Because there is still a considerable lack of experimental excitation functions for cosmogenically relevant reactions, also the capability of nuclear reaction theories to predict unknown excitation functions is of actual interest. Therefore, we have compared our experimental data with "a priori" calculations applying the hybrid model of Blann [5]using the code OVERLAID ALICE [6]. While for the p-induced reactions in the energy region up to 45 MeV the hybrid model is very successful in predicting unknown excitation functions [e.g. 7], for α-induced reactions this is only true with severe restrictions. So the (α,p2n)-, (α,2pn)-, (α,2p3n)-, (α, 2p4n)-, (α,3pn)- and (α,4p3n)-reactions are not adequately described by this theory because of the contribution of incomplete α-break-up and/or other direct reactions. As an example, in Fig.1 the excitation function for the production of ^{57}Ni from Ni is presented which is dominated by the ^{58}Ni(α,2p3n)-reaction. The discrepancies between 30 and 60 MeV can be attributed to the neglect of preequilibrium emission of α-particles. However, above 80 MeV the deviation between theory and experiment rather should be due to a direct knock-out of a single neutron by the impinging α-particle. On the other hand, for (α,xn)-reactions and for those reactions leading to products far away from the target nuclides, the "a priori" calculations agree quite well with the experimental data, as it is shown in Fig.2.

References

[1] R.Michel, G.Brinkmann, H.Weigel and W.Herr,Nucl.Phys.A 322(1979) 40

[2] R.Michel, G.Brinkmann, Nucl.Phys.A 338 (1980) 167

[3] G.Brinkmann, Thesis, University of Cologne (1980)

[4] G.Brinkmann, R.Michel, to be published

[5] M.Blann, Phys.Rev.Letters 27 (1971) 337

[6] M.Blann (1978) UR-NSRL-181

[7] R.Michel, G.Brinkmann, J.Radioanal.Chem. 59 (1980) 467

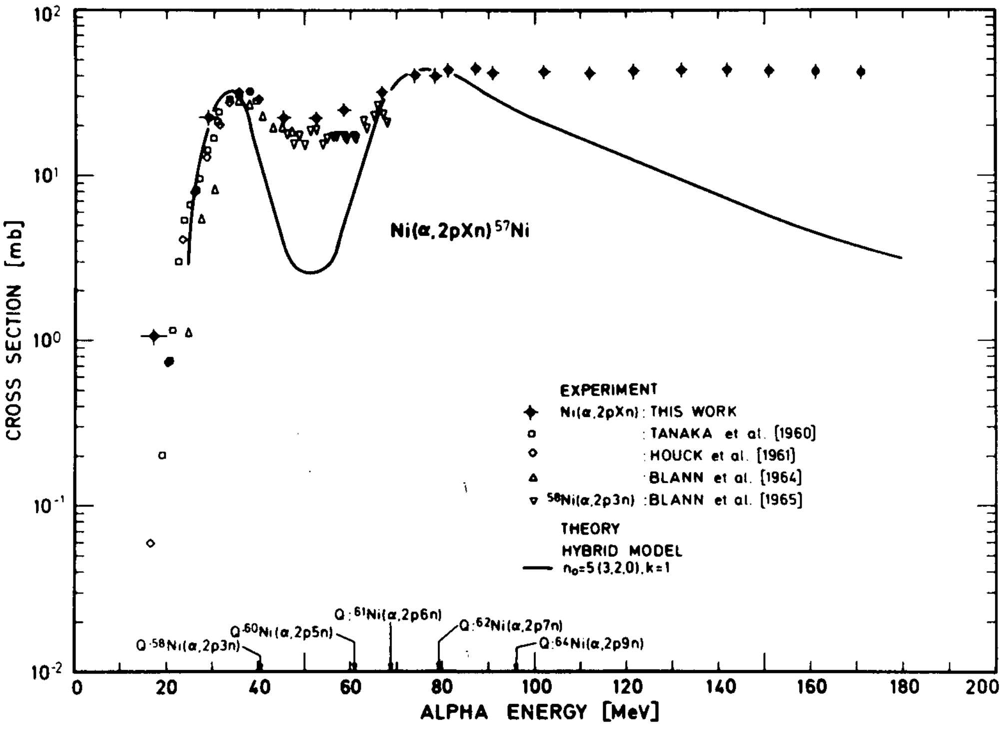

Fig.1 Experimental cross sections and hybrid model calculations for the production of ^{57}Ni from Ni. For a detailed discussion and for references of the work of other authors see [3].

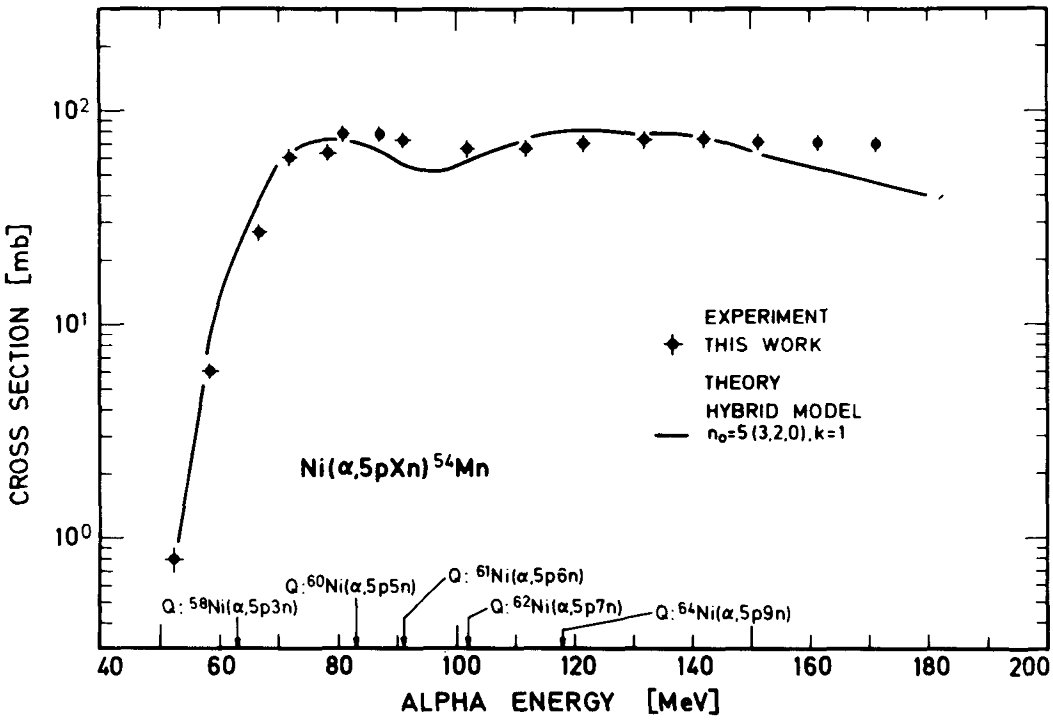

Fig.2 Experimental excitation function and hybrid model calculation for the production of ^{54}Mn from Ni.

FACHBEREICH ANORG. CHEMIE UND KERNCHEMIE
TECHNISCHE HOCHSCHULE DARMSTADT

Triton Formation in Light Charged Particle Induced Nuclear Reactions*

M. Merkel, H. Münzel

Cross sections for the formation of tritons in light charged particle induced reactions were determined |1,2|. The target materials Al, V, Nb and Au were used to characterize reactions of light, medium and heavy nuclides. Thick targets were irradiated with protons, deuterons, helium-3, alpha-particles and Li-6 at the Karlsruhe Isochronous Cyclotron and with protons and deuterons in the upper energy region at the Jülich Isochronous Cyclotron (JULIC).

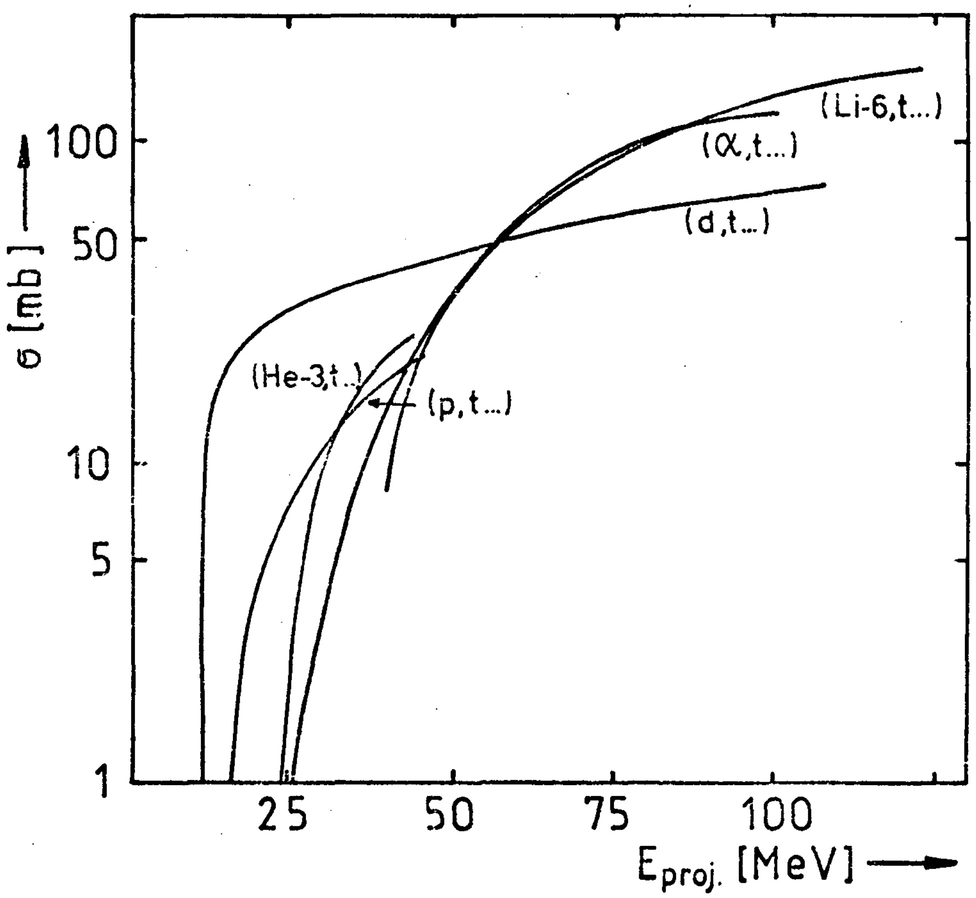

Fig. 1: Excitation-functions for Au(x,t...)-reactions

* Supported by the Bundesministerium für Forschung und Technologie, Federal Republic of Germany and the Nuclear Research Centers in Karlsruhe and Jülich.

The tritium activities, formed in the nuclear reactions, were determined by heat extraction and measurement of the β^--radiation in the gas phase. From the measured thick target-yields excitation functions for (x,t...)-reactions were deduced. The excitation functions for a given projectile are nearly independent of the type of target material. However, for different projectiles considerable deviations are observed as can be seen in Fig. 1.

The highest cross sections are measured in the reactions with α-particles and Li-6. In the case of the α-particles presumedly stripping reactions are the favored reaction channel. The same process contributes also to the Li-6 cross-sections but the reactions may also be induced by particles from a previous projectile break up.

The excitation functions for deuteron induced reactions show another trend. At lower energies they increase much faster than the curves with other projectiles but at higher energies they reach only values of about 40% of the values of α induced reactions. Pick up of a single neutron is probably the major reaction mechanism.

As can be seen in Fig. 1 the probability for triton formation in proton and He-3 induces reactions is considerably lower. In both cases the reaction cannot happen through pick up or stripping of a single nucleon. In He-3 reactions at least one nucleon exchange is necessary. In case of proton reactions two neutrons have to be picked up, i.e. at least two interactions between the nuclei in the composite system must take place to form tritons.

Excitation functions calculated using the exciton model of nuclear reactions |3| are in reasonable agreement with the experimental data.

References

|1| M. Merkel, H. Münzel,
Formation of tritium in nuclear reactions induced by deuterons and α-particles,
Nucl. Phys. A333 (1980) 173.

|2| M. Merkel, H. Münzel,
(p,t...), (d,t...) and (α,t...)-cross sections for Al, V, Nb and Au,
NEANDC(E)-212 U Vol. V (1980) 55.

|3| M. Merkel, H. Münzel,
to be published.

REAKTORSTATION GARCHING; FACHBEREICH PHYSIK
TECHNISCHE UNIVERSITÄT MÜNCHEN

1. Coherent Neutron Scattering Lengths

L. Koester, K. Knopf, J. Meier

Coherent neutron scattering lengths for the bound atoms of seperated isotopes with nucleon number between A = 79 and A = 96 were measured by means of the Christiansen filter technique [1] .
The following results are available at present [2] :

$b(^{79}Br) = 6.79 \pm 0.07$ fm
$b(^{81}Br) = 6.78 \pm 0.07$ fm
$b(^{85}Rb) = 7.07 \pm 0.10$ fm
$b(^{86}Sr) = 5.68 \pm 0.05$ fm
$b(^{87}Sr) = 7.41 \pm 0.07$ fm
$b(^{87}Rb) = 7.27 \pm 0.12$ fm
$b(^{88}Sr) = 7.16 \pm 0.06$ fm
$b(^{89}Y) = 7.75 \pm 0.02$ fm; $b_+ = 8.4 \pm 0.2$ fm, $b_- = 5.8 \pm 0.5$ fm
$b(^{90}Zr) = 6.5 \pm 0.1$ fm
$b(^{91}Zr) = 8.8 \pm 0.1$ fm; $b_+ = 7.9 \pm 0.2$ fm, $b_- = 10.1 \pm 0.2$ fm
$b(^{92}Zr) = 7.5 \pm 0.2$ fm
$b(^{94}Zr) = 8.3 \pm 0.2$ fm
$b(^{96}Zr) = 5.5 \pm 0.1$ fm

Further Christiansen filter experiments were carried out on filters containing thin wires of Au and Pt.

2. Neutron Cross Sections and Resonance Parameters

L. Koester, W. Waschkowski, K. Knopf

Exact measurements of the scattering cross sections at "zero energy" and data of the coherent scattering lengths are necessary for the determination of the incoherent scattering lengths. From these quantities the fundamental spin scattering lengths b_+ and b_- were obtained. They are related to the potential scattering radius R'

and the resonance scattering length b_r according to

$$b_{\pm} = R' + b_{r\pm}$$

$b_{r\pm}$ can be calculated with the known resonance parameters for the parallel (+) and antiparallel (-) orientations of the neutron- and nucleus spin. Precise values of the "zero energy" scattering cross section σ_o have been deduced from measurements of the total cross sections at 1.2 eV and 5.2 eV neutron energy for the ordinary elements Ca, Mn, Br, Rb, Sr, Y and Zr. We have found (for the free nuclei):

$$\sigma_o(\mathrm{Br}) = 5.9 \pm 0.1\ \mathrm{b}\ ; \quad \sigma_{inc} = 0.2 \pm 0.1\ \mathrm{b}$$
$$\sigma_o(\mathrm{Rb}) = 6.24 \pm 0.04\ \mathrm{b}; \quad \sigma_{inc} \simeq 0.001\ \mathrm{b}$$
$$\sigma_o(\mathrm{Sr}) = 6.15 \pm 0.10\ \mathrm{b}; \quad \sigma_{inc} = 0.026 \pm 0.04\ \mathrm{b}$$
$$\sigma_o(\mathrm{Zr}) = 6.52 \pm 0.06\ \mathrm{b}; \quad \sigma_{inc} = 0.12 \pm 0.02\ \mathrm{b}$$

Taking account of all experimental results and resonances parameters we could conclude that the neutron-nucleus interaction at low neutron energies is dominated by bound levels in the cases of

^{79}Br (E_o = -8 eV; J = 1, Γ_γ = 330 meV, Γ_n^o = 8 meV, R'= 7.2 fm)
^{85}Rb ($E_o \simeq$ -20 eV; J = 2, Γ_γ = 220 meV, Γ_n^o = 7.4 meV, R'= 7.2 fm)
^{87}Rb ($E_o \simeq$ -90 eV; J = 1, Γ_γ = 140 meV, Γ_n^o = 24 meV, R'= 7.1 fm),
^{89}Y, ^{91}Zr, ^{92}Zr and ^{94}Zr.

References

[1] L. Koester, Neutron Scattering Lengths and Fundamental Neutron Interactions.
Springer Tracts in Modern Physics, Vol.80, pp1-55
Berlin, Heidelberg, New York: Springer 1977.

[2] L. Koester, K. Knopf. W. Waschkowski:
to be published in Z.Physik A (1981).

PHYSIKALISCH-TECHNISCHE BUNDESANSTALT
BRAUNSCHWEIG

1. Radionuclide Data

Gamma-Ray Emission Probabilities

K. Debertin, U. Schötzig

Gamma-ray emission probabilities p of serveral nuclides were determined by using activity-calibrated sources and germanium spectrometers. For ^{125}Sb relative emission probabilities p_r are given; by multiplying these values with 0.00305(3) emission probabilities p per decay are obtained. For the 909 keV gamma-transition in ^{89}Sr the p-value given in the literature is wrong by a factor of 10.

The given uncertainties in Table I and Table II correspond to one standard deviation and include systematic uncertainties.

2. Neutron Cross Sections

The Covariance File of ENDF/B-V

W. Mannhart

While the $\sigma(E)$-data can immediately be read from the ENDF/B-V file, the same is not true for the covariances. Due to a large flexibility [1] in the structure of the covariance file ("File 33") the information of a single neutron reaction is distributed over various subfiles. A final covariance matrix can only be obtained with regard to all these subfiles. Until now no official processing code is available. On the other hand there is a strong need of applying the uncertainty information as soon as possible for reactor dosimetry purposes. Therefore codes have been written to generate easily understandable sample outputs of the covariance information. An example is given in Table III. The present work comprises the "Dosimetry File" (Tape 531) of ENDF/B-V. The data are available upon request. A report is in progress.

3. Variable Energy Cyclotron and Fast Neutron TOF-Spectrometer

The experimental set up of the PTB-multi-angle time-of-flight (tof) spectrometer for neutron scattering experiments in the energy range $6\ \mathrm{MeV} \leq E_n \leq 14\ \mathrm{MeV}$ has been investigated regarding the neutron source properties and the response of liquid scintillators NE 213 to monoenergetic neutrons.

(a) Characteristic parameters of the $D(d,n)^3He$ neutron source using gas targets

H. Klein, H.J. Brede, B.R.L. Siebert

The angular dependence of the energy width of neutrons produced in gas targets via the reaction $D(d,n)^3He$ has been investigated by analytical approximation, Monte-Carlo simulations and tof-experiments. The effective energy width ΔE_d (FWHM) of the projectile is calculated on the basis of the Bethe-Bloch stopping power formula and appropriate models for the energy straggling. The angular dependent neutron tof-width is additionally sensitive to the angle straggling parameter $\Delta\vartheta_n$ (FWHM). The experimental data for various projectile energies and target entrance foils confirm numerical calculations using extended theories for the multiple small angle scattering in the entrance window of the gas target. As the reaction is strongly pronounced in the forward direction this angle straggling has to be considered in the analysis of scattering experiments as well as in absolute fluence measurements.

(b) Measurement of the $^{12}C(n,\alpha_0)^9Be$ cross section

G. Dietze, H.J. Brede, H. Klein, H. Schölermann

For neutron energies $E_n \geq 6$ MeV the efficiency of organic scintillation detectors is strongly influenced by the neutron-carbon interaction especially if low thresholds in the pulse height spectra are used. Therefore a measurement of the $^{12}C(n,\alpha_0)^9Be$ cross section has been carried out by means of neutron time-of-flight spectroscopy with a NE 213 liquid scintillation detector.

Using a small time-of-flight window and an energy threshold of about 100 keV for recoil protons the α particle spectrum from the reaction $^{12}C(n,\alpha_o)^9Be$ induced by monoenergetic neutrons within the scintillator has been measured. Since the ratio of the carbon and hydrogen content in the scintillator is well known the detector serves as its own neutron fluence monitor. The $^{12}C(n,\alpha_o)^9Be$ cross section can be determined by comparing the pulse height spectra of the detector with theoretical spectra calculated by Monte-Carlo methods. Because of the resonance structure of the reaction cross section near 9.4 MeV the excitation function has been carefully measured in energy steps of 200 keV with a resolution of about 100 keV.

A preliminary analysis shows a significant difference to the evaluated data (published in ENDF-B IV). The final analysis including the angular distribution is in progress.

Table I. Gamma-ray emission probabilities p per decay

Nuclide	Energy in keV	p
^{56}Co	846.7	0.999(7)
	977.4	0.0143(3)
	1037.8	0.1412(14)
	1175.1	0.0227(3)
	1238.3	0.668(6)
	1360.2	0.0426(3)
	1771.4	0.1551(16)
	2015.3	0.0301(7)
	2034.9	0.0787(15)
	2598.5	0.1716(30)
	3202.2	0.0323(11)
	3253.5	0.0795(31)
	3273.2	0.0186(8)
	3451.4	0.0096(5)
^{89}Sr	909	0.0000976(20)
^{232}Th	129.1	0.0223(14)
	209.4	0.0381(11)
	238.6	0.435(12)
	241.0	0.0404(17)
	270.3	0.0344(9)
	277.4	0.0233(7)
	300.1	0.0327(9)
	328.0	0.0310(9)
	338.4	0.1126(27)
	409.4	0.0195(7)
	463.0	0.0450(12)
	583.1	0.307(8)
	727.0	0.0735(20)
	772.1	0.0145(6)
	785.4	0.0107(5)
	794.8	0.0434(11)
	860.4	0.0455(12)
	911.1	0.266(7)
	964.6	0.0505(14)
	968.9	0.1623(38)
	1587.9	0.0326(10)
	2614.6	0.356(11)

Table II. Relative gamma-ray emission probabilities p_r

Nuclide	Energy in keV	p_r
^{125}Sb	116.9	0.872(24)
	172.6	0.66(3)
	176.3	22.8(3)
	204.1	1.09(3)
	208.0	0.796(22)
	227.8	0.452(16)
	321.1	1.400(23)
	380.4	5.04(5)
	408.0	0.603(22)
	427.9	100.0(10)
	443.5	1.023(20)
	463.4	35.1(4)
	600.6	59.0(7)
	606.7	16.78(20)
	636.0	37.6(3)
	671.5	6.04(5)

Table III. Sample output of ENDF/B-V covariances

Reaction: $^{27}Al(n,\alpha)$ MAT = 6313 MT = 107

Reaction threshold: 3.25 MeV

Neutron energy range in eV from	to	Relative uncertainty of σ(E) in %	Correlation matrix (lower triangle only)													
1.00E-5	3.25E+6	0.0	100													
3.25E+6	3.50E+6	50.0	0	100												
3.50E+6	4.00E+6	44.7	0	72	100											
4.00E+6	4.50E+6	24.5	0	65	73	100										
4.50E+6	5.00E+6	21.9	0	73	82	75	100									
5.00E+6	5.50E+6	11.4	0	56	63	58	64	100								
5.50E+6	6.00E+6	9.9	0	64	72	66	73	57	100							
6.00E+6	7.00E+6	7.8	0	61	69	63	70	54	62	100						
7.00E+6	8.00E+6	7.2	0	67	74	68	76	59	67	64	100					
8.00E+6	9.00E+6	6.7	0	72	80	73	82	63	72	69	74	100				
9.00E+6	1.00E+7	5.8	0	69	77	70	78	60	69	66	71	77	100			
1.00E+7	1.20E+7	5.6	0	72	80	73	82	63	72	69	75	80	77	100		
1.20E+7	1.50E+7	5.0	0	0	0	0	0	0	0	0	0	0	0	0	100	
1.50E+7	2.00E+7	5.0	0	0	0	0	0	0	0	0	0	0	0	0	0	100

References

[1] F.G. Perey, ORNL/TM-5938 (1978)

INSTITUT FUER KERNCHEMIE

PHILIPPS-UNIVERSITÄT MARBURG

1. Gamma-Ray Catalog

U. Reus, W. Westmeier, I. Warnecke[+]

Quantitative information on gamma rays from the decay of radioactive nuclides is required in many areas of nuclear science as well as related fields. We have therefore produced a compilation of the decay properties of all known radionuclides, with the main emphasis on energies and absolute intensities of gamma rays.

The most recent version of the catalog was issued in 1979 and includes references through June 1978. It covers data on 2311 nuclides and isomers with a total of more than 35,000 gamma energies. In PART I of the catalog the gamma rays are listed in order of increasing energy, this part being designed for the identification of unknown gamma lines. In PART II the complete data-sets for each nuclide are listed in order of mass number A and nuclear charge Z of the nuclides. This part also contains additional information, references, and comments in case of any discrepancies.
This issue of the catalog is out of print for the time being, and no more copies are available. Updating is in progress, and references through December 1980 will be included. The revised version of the catalog will be published in the near future in an appropriate journal and will the be available for all interested research groups.

2. Alpha-Energy Table

W. Westmeier, R.A. Esterlund

A compilation of alpha-decay properties of all known alpha-emitting nuclides, which includes data on alpha energies, intensities and the abundance of the alpha branch, is permanently being updated. The table is ordered by increasing energy and covers data on 528 alpha emitters with a total of 1592 energies at present.
Computer printout copies of the table are available on request.

[+]Physikalisch-Technische Bundesanstalt, Braunschweig

FACHINFORMATIONSZENTRUM ENERGIE PHYSIK MATHEMATIK

Status Report

H. Behrens, J.W. Tepel

1. Information System für Physics Data in the Federal Republic of Germany

This project has been described earlier in the Progress Reports NEANDC (E) - 172 U Vol. V, NEANDC (E) - 182 U Vol. V and NEANDC (E) - 192 U Vol. V. No details are therefore given here.

2. New Data compilations

The following new issues in the series Physics Data were published in the meantime:

5-1o (198o):	Gases and Carbon in Metals (Thermodynamics, Kinetics and Properties) Part X: Group VIA Metals (1): Chromium, Tungsten H. Jehn, H. Speck, E. Fromm and G. Hörz
5-11 (198o):	Gases and Carbon in Metals (Thermodynamics, Kinetics and Properties) Part XI: Group VIA Metals (2): Molybdenum H. Jehn, H. Speck, E. Fromm and G. Hörz
13-2:	Evaluation of the cross sections for the reactions ^{19}F (n,2n) ^{18}F, ^{31}P (n,p) ^{31}Si, ^{93}Nb and ^{1o3}Rh (n,n') ^{1o3}Rh B. Strohmaier, S. Tagesen and H. Vonach
17-1 (1981)	Compilation of Experimental Values of Internal Conversion Coefficients and Ratios for Nuclei with $Z < 6o$. H.H.Hansen

13-3 (1981): in preparation

3. Bibliographic of Existing Data Compilations

The corresponding database INKA-Datacomp has been updated in the meantime. A new completed printed issue of the whole bibliography is in preparation.

4. The Evaluated Nuclear Structure Data Files (ENSDF)

In the past year the mass chains were published viz. A = 85, 91 and 92 [1,2,3]. Two further mass chains A = 95, 96, have been completed and are in the review procedure. The mass chains A = 93, 97 and 98 are in preparation.

In the last year the database management system/ADABAS/NATURAL was introduced at the FIZ. Thus, ENSDF and the corresponding bibliographic files NSR was loaded under the database management system above mentioned. The advantage is an easy retrieval and updating of both databases.

As an application a systematic study of logft-values in ß-decay was performed [4].

References

[1] J.W. Tepel, Nuclear Data Sheets für A = 85, Nuclear Data Sheets 3o, 5o1 (198o)
[2] H.W. Müller, Nuclear Data Sheets für A = 91, Nuclear Data Sheets, 31, 181 (198o)
[3] P. Luksch, Nuclear Data Sheets für A = 92, Nuclear Data Sheets 3o, 573 (198o)
[4] H. Behrens, P. Luksch,H.W.Müller, J.W. Tepel, Systemmatics of the international Conference on Nuclear Physics, Berkeley (198o).

APPENDIX

Addresses of Contributing Laboratories

Institut für Angewandte Kernphysik II
Director: Prof.Dr. G. Schatz
Senior reporters: Dr. S. Cierjacks
Dr. F. Käppeler
Kernforschungszentrum Karlsruhe
Postfach 3640
7500 Karlsruhe

Institut für Kernphysik II
Director: Prof.Dr. A. Citron
Senior reporter: Dr. S. Cierjacks
Kernforschungszentrum Karlsruhe
Postfach 3640
7500 Karlsruhe

Institut für Kern- und Teilchenphysik
Director: Prof.Dr. B. Zeitnitz
Senior reporter: Dr. H.-O. Klages
Kernforschungszentrum Karlsruhe
Postfach 3640
7500 Karlsruhe

Institut für Neutronenphysik und Rektortechnik
Director: Dr. G. Kessler
Senior reporter: Dr. F.H. Fröhner
Kernforschungszentrum Karlsruhe
Postfach 3640
7500 Karlsruhe

Institut für Chemie (1): Nuklearchemie
Director: Prof.Dr. G. Stöcklin
Senior reporter: Dr. S.M. Qaim
Kernforschungsanlage Jülich
Postfach 1913
5170 Jülich

I. Institut für Experimentalphysik
Director: Prof.Dr. H. Neuert
Senior reporter: Prof.Dr. W. Scobel
Universität Hamburg
Luruper Chaussee 149
2000 Hamburg 50

Institut für Reine und Angewandte
Kernphysik
Director: Prof.Dr. K.O. Thielheim
Senior reporter: Dr. H.G. Priesmeyer
Universität Kiel, Geesthacht
Reaktorstr. 1
2054 Geesthacht/Tesperhude

Institut für Kernchemie
Director: Prof.Dr. W. Herr
Senior reporter: Dr. G. Brinkmann
Universität zu Köln
Zülpicher Str. 47
5000 Köln

Fachbereich Anorganische Chemie
und Kernchemie
Senior reporter: Prof.Dr. H. Münzel
Technische Hochschule Darmstadt
Hochschulstr.
61000 Darmstadt

Fachbereich Physik der
Technischen Universität München
Abteilung E14, Forschungsreaktor
Head and senior reporter: Prof.Dr. L. Köster
8046 Garching/München

Physikalisch-Technische Bundesanstalt
Abteilung 6, Atomphysik
Director: Prof.Dr. S. Wagner
Senior reporter: Dr. W. Mannhart
Bundesallee 100
3300 Braunschweig

Institut für Kernchemie
Senior reporter: Prof.Dr. P. Patzelt
Philipps-Universität Marburg
Lahnberge
3550 Marburg/Lahn

Fachinformationszentrum Energie, Physik, Mathematik
Directors: Dr. W. Rittberger, E.-O. Schulze
Senior reporter: Dr. H. Behrens
Kernforschungszentrum
7514 Eggenstein-Leopoldshafen 2

CINDA TYPE INDEX

A Supplement to Progress Report on
Nuclear Data Research in the Federal
Republic of Germany for the Period
April 1, 1980 to March 31, 1981

NEANDC(E)-222 U Vol. V
INDC (Ger)-23/L + Special
FIZ-KA-2

ELEMENT S	A	QUANTITY	TYPE	ENERGY MIN	MAX	DOCUMENTATION REF	VOL	PAGE	DATE	LAB	COMMENTS
MA	NY	N,DEUTERON	EXPT-PROG	15+7		NEANDC(E)-222U			781	JUL	VOL.5.P.30.QAIM+ ND+NNP,VS(N-Z)/A
LI	007	N,N TRITON	EXPT-PROG	40+6	10+7	NEANDC(E)-222U			781	KIG	VOL.5.P.32.LISKIEN+ TBC,EXCIT-FN,NDG
B	010	TOTAL	EXPT-PROG	15+6	40+7	NEANDC(E)-222U			781	KFK	VOL.5.P.21.ABDEL-WAHAB+ ABST,NDG
B	011	TOTAL	EXPT-PROG	15+6	40+7	NEANDC(E)-222U			781	KFK	VOL.5.P.21.ABDEL-WAHAB+ ABST,NDG
C	012	RESON PARAMS	EXPT-PROG	37+4	15+5	NEANDC(E)-222U			781	KFK	VOL.5.P.13.CIERJACKS+ ISOSPIN MIXING
C	012	N,ALPHA	EXPT-PROG	+6	+7	NEANDC(E)-222U			781	PTB	VOL.5.P.59.KLEIN+SIG,EXCIT-F,TBC,NDG
O	016	RESON PARAMS	EXPT-PROG	74+6	15+7	NEANDC(E)-222U			781	KFK	VOL.5.P.10.HINTERBERGER+TBL RES PARS
O	016	RESON PARAMS	EXPT-PROG	16+4	34+5	NEANDC(E)-222U			781	KFK	VOL.5.P.13.CIERJACKS+ ISOSPIN MIXING
NE	020	N,GAMMA	EXPT-PROG	30+3	20+5	NEANDC(E)-222U			781	KFK	VOL.5.P.1 ALMEIDA+ TOF,NDG,TBC
NE	020	RESON PARAMS	EXPT-PROG	15+6	40+7	NEANDC(E)-222U			781	KFK	VOL.5.P.22 ABDEL-WAHAB+ ABST,NDG
NE	020	TOTAL	EXPT-PROG	15+6	40+7	NEANDC(E)-222U			781	KFK	VOL.5.P.22 ABDEL-WAHAB+ ABST,NDG
NE	020	TOTAL	EXPT-PROG	70+3	80+5	NEANDC(E)-222U			781	KFK	VOL.5.P.1.ALMEIDA+ TRANS TOF,GRPHS
NE	021	N,GAMMA	EXPT-PROG	30+3	20+5	NEANDC(E)-222U			781	KFK	VOL.5.P.1 ALMEIDA+ TOF,NDG,TBC
NE	021	TOTAL	EXPT-PROG	70+3	80+5	NEANDC(E)-222U			781	KFK	VOL.5.P.1 ALMEIDA+ TRANS TOF,GRPHS
NE	022	N,GAMMA	EXPT-PROG	30+3	20+5	NEANDC(E)-222U			781	KFK	VOL.5.P.1 ALMEIDA+ TOF,NDG,TBC
NE	022	TOTAL	EXPT-PROG	70+3	80+5	NEANDC(E)-222U			781	KFK	VOL.5.P.1 ALMEIDA+ TRANS TOF,GRPHS
AL	027	N,TRITON	EXPT-PROG		30+7	NEANDC(E)-222U			781	JUL	VOL.5.P.29 QAIM+ INTEG-SIG,CFD CALC
AL	027	RESON PARAMS	EXPT-PROG	35+4		NEANDC(E)-222U			781	KFK	VOL.5.P.2 WISSHAK+ WG, S-WAVE,TBC
CA	044	N,DEUTERON	EXPT-PROG	15+7		NEANDC(E)-222U			781	JUL	VOL.5.P.30.QAIM+ ND+NNP SIG
TI	049	N,DEUTERON	EXPT-PROG	15+7		NEANDC(E)-222U			781	JUL	VOL.5.P.30.QAIM+ ND+NNP SIG
CR	050	N,DEUTERON	EXPT-PROG	15+7		NEANDC(E)-222U			781	JUL	VOL.5.P.30.QAIM+ ND+NNP SIG
CR	053	N,HELIUM3	EXPT-PROG		30+7	NEANDC(E)-222U			781	JUL	VOL.5.P.29.QAIM+ INTEG SIG,CFD CALC
V	051	N,HELIUM3	EXPT-PROG		30+7	NEANDC(E)-222U			781	JUL	VOL.5.P.29.QAIM+ INTEG SIG,CFD CALC
FE	056	N,TRITON	EXPT-PROG		30+7	NEANDC(E)-222U			781	JUL	VOL.5.P.29.QAIM+ INTEG SIG,CFD CALC
FE	056	RESON PARAMS	EXPT-PROG	28+4		NEANDC(E)-222U			781	KFK	VOL.5.P.2.WISSHAK+ WG, S-WAVE,TBC
FE	056	RESON PARAMS	EXPT-PROG	10+4	10+5	NEANDC(E)-222U			781	KFK	VOL.5.P.3.KAEPPELER+ WG,NDG
FE	058	N,GAMMA	EXPT-PROG	36+4	70+4	NEANDC(E)-222U			781	KFK	VOL.5.P.3 KAEPPELER+ GRAPH,ANAL TBC
FE	058	RESON PARAMS	EXPT-PROG	36+4	70+4	NEANDC(E)-222U			781	KFK	VOL.5.P.3 KAEPPELER+ WG,NDG,TBC
CO	059	N,TRITON	EXPT-PROG		30+7	NEANDC(E)-222U			781	JUL	VOL.5.P.29.QAIM+ INTEG SIG,CFD CALC
NI	058	RESON PARAMS	EXPT-PROG	16+4		NEANDC(E)-222U			781	KFK	VOL.5.P.2 WISSHAK+ WG, S-WAVE,TBC
NI	060	RESON PARAMS	EXPT-PROG	13+4		NEANDC(E)-222U			781	KFK	VOL.5.P.2 WISSHAK+ WG, S-WAVE,TBC
ZN	067	N,DEUTERON	EXPT-PROG	15+7		NEANDC(E)-222U			781	JUL	VOL.5.P.30.QAIM+ ND+NNP SIG
ZN	068	N,DEUTERON	EXPT-PROG	15+7		NEANDC(E)-222U			781	JUL	VOL.5.P.30.QAIM+ ND+NNP SIG
BR		THERMAL SCAT	EXPT-PROG	00+0		NEANDC(E)-222U			781	MUN	VOL.5.P.56.KOESTER+ SCAT SIG
BR	079	THERMAL SCAT	EXPT-PROG	NDG		NEANDC(E)-222U			781	MUN	VOL.5.P.56.KOESTER+ COH SCAT LENGTH
BR	079	RESON PARAMS	EXPT-PROG	-8+1		NEANDC(E)-222U			781	MUN	VOL.5.P.56.KOESTER+ TBL RES PARS
BR	081	THERMAL SCAT	EXPT-PROG	NDG		NEANDC(E)-222U			781	MUN	VOL.5.P.56.KOESTER+ COH SCAT LENGTH
RB		THERMAL SCAT	EXPT-PROG	00+0		NEANDC(E)-222U			781	MUN	VOL.5.P.56.KOESTER+ SCAT SIG
RB	085	THERMAL SCAT	EXPT-PROG	NDG		NEANDC(E)-222U			781	MUN	VOL.5.P.56.KOESTER+ COH SCAT LENGTH
RB	085	RESON PARAMS	EXPT-PROG	-2+2		NEANDC(E)-222U			781	MUN	VOL.5.P.56.KOESTER+ TBL RES PARS
RB	087	THERMAL SCAT	EXPT-PROG	NDG		NEANDC(E)-222U			781	MUN	VOL.5.P.56.KOESTER+ COH SCAT LENGTH
RB	087	RESON PARAMS	EXPT-PROG	-9+2		NEANDC(E)-222U			781	MUN	VOL.5.P.56.KOESTER+ TBL RES PARS
SR		THERMAL SCAT	EXPT-PROG	00+0		NEANDC(E)-222U			781	MUN	VOL.5.P.56.KOESTER+ SCAT SIG
SR	086	THERMAL SCAT	EXPT-PROG	NDG		NEANDC(E)-222U			781	MUN	VOL.5.P.56.KOESTER+ COH SCAT LENGTH
SR	087	THERMAL SCAT	EXPT-PROG	NDG		NEANDC(E)-222U			781	MUN	VOL.5.P.56.KOESTER+ COH SCAT LENGTH
SR	088	THERMAL SCAT	EXPT-PROG	NDG		NEANDC(E)-222U			781	MUN	VOL.5.P.56.KOESTER+ COH SCAT LENGTH
Y	089	THERMAL SCAT	EXPT-PROG	NDG		NEANDC(E)-222U			781	MUN	VOL.5.P.56.KOESTER+ COH SCAT LENGTH
ZR		THERMAL SCAT	EXPT-PROG	00+0		NEANDC(E)-222U			781	MUN	VOL.5.P.56.KOESTER+ SCAT SIG
ZR	090	THERMAL SCAT	EXPT-PROG	NDG		NEANDC(E)-222U			781	MUN	VOL.5.P.56.KOESTER+ COH SCAT LENGTH
ZR	091	THERMAL SCAT	EXPT-PROG	NDG		NEANDC(E)-222U			781	MUN	VOL.5.P.56.KOESTER+ COH SCAT LENGTH
ZR	092	N,DEUTERON	EXPT-PROG	15+7		NEANDC(E)-222U			781	JUL	VOL.5.P.30.QAIM+ ND+NNP SIG
ZR	092	THERMAL SCAT	EXPT-PROG	NDG		NEANDC(E)-222U			781	MUN	VOL.5.P.56.KOESTER+ COH SCAT LENGTH
ZR	094	THERMAL SCAT	EXPT-PROG	NDG		NEANDC(E)-222U			781	MUN	VOL.5.P.56.KOESTER+ COH SCAT LENGTH
ZR	096	THERMAL SCAT	EXPT-PROG	NDG		NEANDC(E)-222U			781	MUN	VOL.5.P.56.KOESTER+ COH SCAT LENGTH
NB	093	N,TRITON	EXPT-PROG		30+7	NEANDC(E)-222U			781	JUL	VOL.5.P.29.QAIM+ INTEG SIG,CFD CALC
NB	093	N,GAMMA	EXPT-PROG	10+4	70+4	NEANDC(E)-222U			781	KFK	VOL.5.P.7.REFFO+ REL AU197,ABST,NDG
MO	097	N,DEUTERON	EXPT-PROG	15+7		NEANDC(E)-222U			781	JUL	VOL.5.P.30.QAIM+ ND+NNP SIG
MO	098	N,DEUTERON	EXPT-PROG	15+7		NEANDC(E)-222U			781	JUL	VOL.5.P.30.QAIM+ ND+NNP SIG

ELEMENT S A	QUANTITY	TYPE	ENERGY MIN	MAX	DOCUMENTATION REF	VOL	PAGE	DATE	LAB	COMMENTS
RH 103	N,GAMMA	EXPT-PROG	10+4	70+4	NEANDC(E)-222U			781	KFK	VOL.5.P.7.REFFO+ REL AU197,ABST,NDG
XE 124	N,GAMMA	EXPT-PROG	25+4		NEANDC(E)-222U			781	KFK	VOL.5.P.5 BEER+ 1134 MB, REL AU-197
XE 132	N,GAMMA	EXPT-PROG	25+4		NEANDC(E)-222U			781	KFK	VOL.5.P.5 BEER+ 69 MB, REL AU-197
XE 134	N,GAMMA	EXPT-PROG	25+4		NEANDC(E)-222U			781	KFK	VOL.5.P.5 BEER+ 34 MB, REL AU-197
CS	RESON PARAMS	EXPT-PROG	42+1	88+2	NEANDC(E)-222U			781	KIG	VOL.5.P.48.PRIESMEYER+ EN,GRAPHS
EU 151	N,GAMMA	EXPT-PROG	25+4		NEANDC(E)-222U			781	KFK	VOL.5.P.5 BEER+ 2051 MB, REL AU-197
SM 152	N,GAMMA	EXPT-PROG	25+4		NEANDC(E)-222U			781	KFK	VOL.5.P.5 BEER+ 440 MB, REL AU-197
GD 152	N,GAMMA	EXPT-PROG	25+4		NEANDC(E)-222U			781	KFK	VOL.5.P.5 BEER+ 1144 MB, REL AU-197
GD 158	N,GAMMA	EXPT-PROG	25+4		NEANDC(E)-222U			781	KFK	VOL.5.P.5 BEER+ 242 MB, REL AU-197
GD 160	N,GAMMA	EXPT-PROG	25+4		NEANDC(E)-222U			781	KFK	VOL.5.P.5.BEER+ 159 MB, REL AU-197
TA 181	N,GAMMA	EXPT-PROG	10+4	70+4	NEANDC(E)-222U			781	KFK	VOL.5.P.7.REFFO+ REL AU197,ABST,NDG
IR 191	RESON PARAMS	EXPT-PROG	65-1		NEANDC(E)-222U			781	KIG	VOL.5.P.46.PRIESMEYER+ EN,WG,GRPH
IR 193	RESON PARAMS	EXPT-PROG	13+0		NEANDC(E)-222U			781	KIG	VOL.5.P.46.PRIESMEYER+ EN,WG,GRPH
U 235	FRAG SPECTRA	EXPT-PROG	50+5	55+6	NEANDC(E)-222U			781	KFK	VOL.5.P.7.MUELLER+ EN-DIST,ABST,NDG
U 235	FISS YIELD	EXPT-PROG	50+5	55+6	NEANDC(E)-222U			781	KFK	VOL.5.P.7 MUELLER+MASSDIST,ABST,NDG
AM 241	N,FISSION	EVAL-PROG	20+3	40+5	NEANDC(E)-222U			781	KFK	VOL.5.P.25 GOEL+ GRAPH
AM 241	N,GAMMA	EVAL-PROG	20+3	40+5	NEANDC(E)-222U			781	KFK	VOL.5.P.25 GOEL+ GRAPH
AM 241	SPECT N,GAMT	EXPT-PROG	15-3	30+4	NEANDC(E)-222U			781	KFK	VOL.5.P.8.WISSHAK+ ISOMERIC RATIO
AM 242	EVALUATION	EVAL-PROG	NDG		NEANDC(E)-222U			781	KFK	VOL.5.P.25 GOEL+ TBC,NDG
AM 243	EVALUATION	EVAL-PROG	NDG		NEANDC(E)-222U			781	KFK	VOL.5.P.25 GOEL+ TBC,NDG
CM 244	EVALUATION	EVAL-PROG	NDG		NEANDC(E)-222U			781	KFK	VOL.5.P.25 GOEL+ TBC,NDG